Pergamon

Journal of Structural Geology, Vol. 20, No. 12, pp. 1747 to 1767, 1998

PII: S0191-8141(98)00084-4
0191-8141/98/$ - see front matter

Three-dimensional strain produced by >50 My of episodic extension, Horse Prairie basin area, SW Montana, U.S.A.

COLBY J. VANDENBURG*, SUSANNE U. JANECKE†

Department of Geology, Utah State University, Logan, UT 84322-4505, U.S.A.

and

WILLIAM C. McINTOSH

New Mexico Bureau of Mines and Mineral Resources, Socorro, NM 87801, U.S.A.

(*Received* 25 *May* 1997; *accepted in revised form* 21 *June* 1998)

Abstract—The Horse Prairie basin of southwestern Montana is a complex, east-dipping half-graben that contains three angular unconformity-bounded sequences of Tertiary sedimentary rocks overlying middle Eocene volcanic rocks. New mapping of the basin and its hanging wall indicate that five temporally and geometrically distinct phases of normal faulting and at least three generations of fault-related extensional folding affected the area during the late Mesozoic (?) to Cenozoic. All of these phases of extension are evident over regional or cordilleran-scale domains. The extension direction has rotated ~90° four times in the Horse Prairie area resulting in a complex three-dimensional strain field with ≫60% east–west and >25% north–south bulk extension. Extensional folds with axes at high angles to the associated normal fault record most of the three-dimensional strain during individual phases of extension (phases 3a, 3b, and 4). Cross-cutting relationships between normal faults and Tertiary volcanic and sedimentary rocks constrain the ages of each distinct phase of deformation and show that extension continued episodically for more than 50 My. Gravitational collapse of the Sevier fold and thrust belt was the ultimate cause of most of the extension. © 1998 Published by Elsevier Science Ltd. All rights reserved

INTRODUCTION

Models of rift basins commonly depict a relatively simple geometry produced during a single, sometimes protracted episode of extension (Gibbs, 1984; Leeder and Gawthorpe, 1987). In recent years, many along-strike variations in geometry have been described (Nielsen and Beratan, 1990; Evans and Oaks, 1996; Faulds and Varga, 1998), and a large body of work now shows that multiple phases of extension affected many extensional terranes (Best, 1988; Gans *et al*., 1989; Taylor *et al*., 1989; Janecke, 1992; Axen *et al*., 1993). In some areas, new normal faults formed at a high angle to pre-existing ones (Zoback *et al*., 1981; Best, 1988; Janecke, 1992), producing a complex three-dimensional bulk strain. In this paper we document the remarkably complex extensional deformation within and adjacent to a seemingly simple half graben (the Horse Prairie half graben) in the U.S. Basin and Range province that resulted from two- and three-dimensional strain during five distinct phases of extension. This type of complexity is not unique to our study area, and is evident in many of the adjacent Paleogene half graben as well as unrelated half graben of the Basin and Range province (Link, 1982; O'Neill and Pavlis, 1988; Silverberg, 1990; Fryxell, 1991; Janecke, 1992; Blankenau and Janecke, 1997; Smith, 1997; Evans and Janecke, 1998).

Previous work southwest and northeast of the Horse Prairie half graben (Fig. 1) documented two to three phases of normal faulting along NE-, NW- and N-striking normal faults. In east-central Idaho, Janecke (1992) described three episodes of Cenozoic extension: Middle Eocene extension along synvolcanic NE-striking normal faults, then Eocene to Oligocene extension along W- to WSW-dipping low-angle normal faults and finally late Cenozoic extension along NW-striking Basin and Range faults. Northeast of the present study area in the Ruby Mountains area, Fritz and Sears (1993) documented an additional episode of extension and half graben formation along NE-striking late-Early Miocene normal faults. The time–space patterns and origins of these four rifting events remain controversial (Fritz and Sears, 1993; Janecke, 1992, 1994; Hanneman, 1989; Constenius, 1996; Sears, 1995) but there is little doubt that each of these events is at least a regional and most likely a cordilleran-wide tectonic event. This study of the Horse Prairie basin area was undertaken in part to determine which of these four rifting events produced the generally east-tilted half grabens of SW Montana and adjacent Idaho (Fig. 1a).

Geologic mapping at a scale of 1:24,000, structural and basin analysis, examination of moderate to poor quality seismic-reflection profiles (figs 12 & 15 in

*Current address: Exxon Exploration and Production, Houston, Texas, U.S.A.
†e-mail: sjanecke@cc.usu.edu

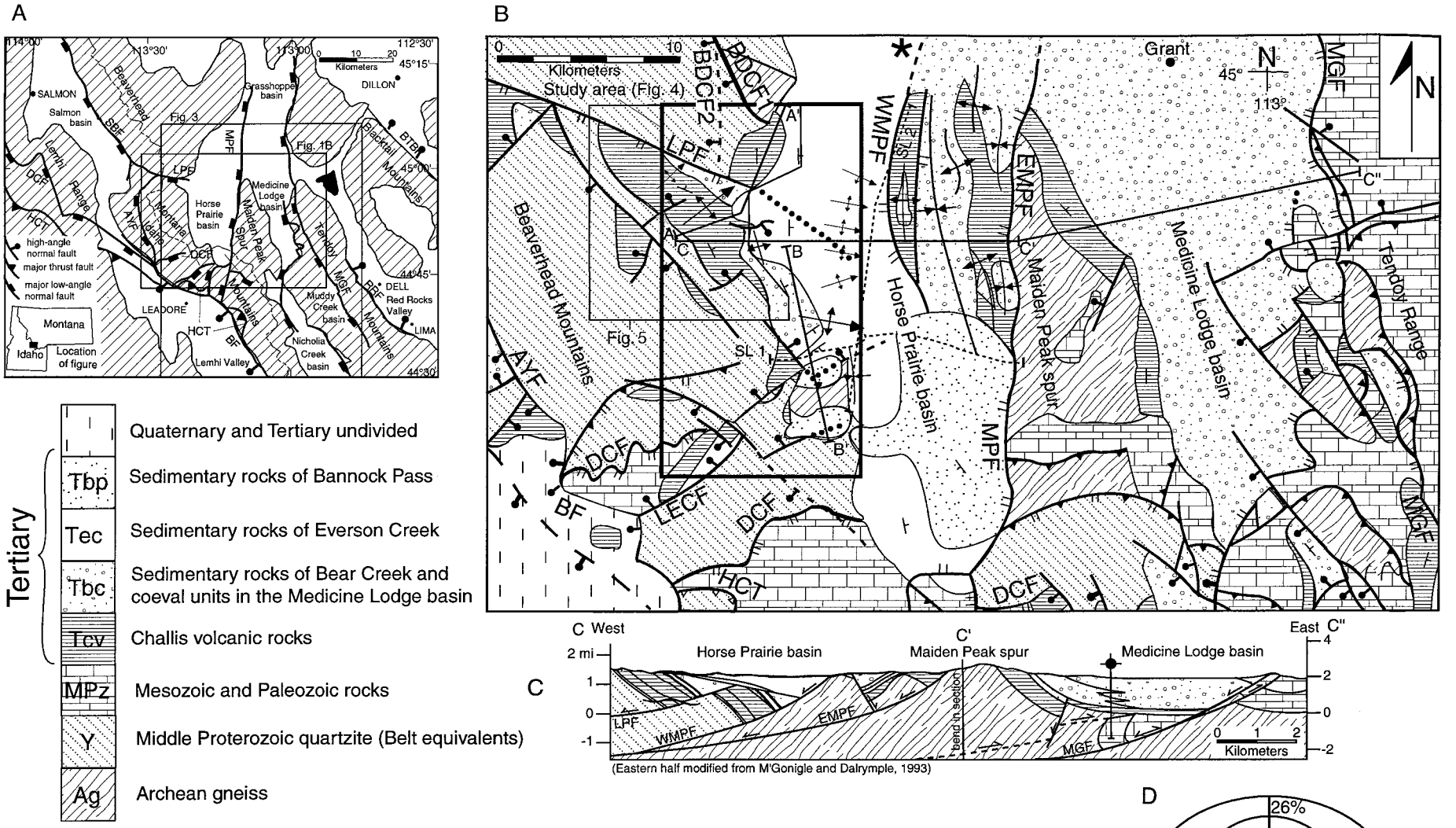

Fig. 1. Simplified geologic map and cross-section of the Horse Prairie and Medicine Lodge basins. (a) Geographic setting of the study area. (b) Map showing the regional setting of the study area. Star denotes a 19.5 ± 1.1 Ma basalt (K–Ar age determination, 49% radiogenic argon, McDowell, Fritz, Wampler, and Sears, personal communication). Geologic map is compiled from Scholten *et al.* (1955), Scholten and Ramspott (1968), Staatz (1973, 1979), Dubois (1982), Hansen (1983), Perry and Sando (1983), Skipp (1988), M'Gonigle *et al.* (1991), M'Gonigle (1993, 1994), M'Gonigle and Hait (1997), VanDenburg (1997), and S. U. Janecke (unpublished mapping). (c) Cross-section across the three main detachment faults formed during phase 3. Compiled from VanDenburg (1997), M'Gonigle and Hait (1997), and M'Gonigle and Dalrymple (1993). Western half is simplified from Fig. 6(c). (d) Post-middle Eocene strain ellipse for the study area. Abbreviations are: Agency–Yearian fault (AYF); Beaverhead fault (BF); Blacktail fault (BTF); older and younger strands of the Bloody Dick Creek fault (BDCF1, BDCF2); Divide Creek fault (DCF); Eastern Maiden Peak fault (EMPF); Hawley Creek thrust (HCT); Lemhi Pass fault (LPF); Little Eightmile Creek fault (LECF); Maiden Peak fault system (MPF); Muddy-Grasshopper fault (MGF); Salmon basin fault (SBF); Red Rocks fault (RRF); seismic lines 1 and 2 (SL1, and SL2); Western Maiden Peak fault (WMPF, Horse Prairie fault of M'Gonigle and Hait, 1997).

VanDenburg, 1997), and geologic cross-sections were used to determine the deformational history and geometry of extension in the Horse Prairie area (Fig. 1). Five $^{40}Ar/^{39}Ar$ age determinations were conducted on samples collected from the oldest Tertiary rocks in the area, the middle Eocene Challis volcanic rocks, and from tuffs intercalated within the overlying syntectonic sedimentary sequence. These critical geochronological data, along with previous biostratigraphic analyses (Fields *et al*., 1985; R. Nichols, unpublished data) were used to assign ages to each of the five distinct phases of extension that deform the area. In this paper we report the results of our geological mapping and structural analysis, and illustrate the sequential development of a three-dimensional strain field. After a brief description of the geological setting, we outline the stratigraphy and age of the Cenozoic volcanic and sedimentary basin-fill deposits. A description of the normal faults and extensional folds formed during each of the five phases of extension follows, along with a discussion of the resulting three-dimensional strain.

LOCAL GEOLOGICAL SETTING

The Horse Prairie half graben lies within the Rocky Mountain Basin and Range province of the U.S. Cordillera (Fig. 1). The basin dips east and contains Tertiary lacustrine, fluvial, and paludal sedimentary rocks, monolithologic breccias, along with volcanic rocks temporally correlated to the 50–45 Ma Challis volcanic group of central Idaho (Figs 1 & 2; M'Gonigle and Dalrymple, 1993). The Maiden Peak spur to the east is bounded on its western flank by a system of north-striking, west-dipping, low-angle normal faults (M'Gonigle, 1994; M'Gonigle and Hait, 1997). The Maiden Peak basin-bounding fault system has exhumed Archean basement rocks overlain by east-tilted Paleozoic and Cenozoic strata. The Beaverhead Mountains to the west of the Horse Prairie basin consist mainly of Middle Proterozoic metasedimentary rocks equivalent to the Belt Supergroup, but also contain Paleozoic sedimentary rocks (Fig. 1b) (Staatz, 1979; Skipp, 1988).

The Paleogene Horse Prairie half graben was superimposed on the Southwest Montana Re-entrant of the Mesozoic to early Tertiary Sevier fold and thrust belt (Fig. 3). The Hawley Creek thrust, one of the largest thrust faults at this latitude, is exposed 7–10 km to the southwest of the study area (Lucchitta, 1966; Ruppel, 1968; Skipp, 1988) (Figs 1a & 3), whereas the frontal thrusts, exposed to the east in the Tendoy Range, project beneath the basin (Fig. 3) (Perry *et al*., 1988; McDowell, 1992, 1997).

A major pre-Eocene fault or system of faults is required beneath the Horse Prairie half graben to explain the lack of Middle Proterozoic metasedimentary rocks (Belt rocks) east of the basin. We infer that the half graben overlies the original rifted margin of the Belt basin, and/or a Mesozoic–Cenozoic thrust fault, because both types of faults project into the half graben from nearby areas (McKenzie, 1949; Coppinger, 1974; Tucker, 1975; Skipp, 1987, 1988; M'Gonigle, 1993, 1994) (Fig. 3). Shortening in this region ended before the middle Eocene Challis volcanic field developed on top of the fold and thrust belt (Harlan *et al*., 1988; Skipp, 1988). The main eruptive centers of the Challis volcanic field are 40–140 km west of the study area.

Crustal extension began in this region by Middle Eocene times and continues today along Basin and Range normal faults (e.g. BF, BTF, and RRF, Fig. 1a). Half graben formed during two of the five major phases of extension to deform this area (Figs 1a, see below), and include ENE-tilted Eocene to Oligocene half graben of phase 3 [Grasshopper, Horse Prairie, Medicine Lodge, Muddy Creek, Nicholia Creek, and Salmon basins (Janecke, 1994)] and NW-trending Late Cenozoic half graben of phase 5 (Lemhi and Red Rocks Valleys, Fig. 1a). NE-trending half graben associated with phase 2 are preserved northwest of the area in Fig. 1(a) along the Trans Challis fault zone (McIntyre *et al*., 1985; Janecke *et al*., 1997), whereas basins associated with phase 4 are preserved to the northeast in the Ruby Mountains area (Fritz and Sears, 1993).

TERTIARY STRATIGRAPHY

The study area (Fig. 1) contains four unconformity-bounded sequences of Tertiary volcanic and sedimentary rocks which are broadly coeval with all but the first generation of normal faults (Figs 2 & 4). Cross-cutting relationships between these four sequences of Tertiary rocks and normal faults and folds were used to establish both the relative sequence and absolute timing of deformational events. Delineating the stratigraphy is critical to determining the age of individual structures, so we briefly describe the Tertiary rock units. More detailed descriptions of these rock units are in VanDenburg (1997). Thicknesses of Tertiary rock units were estimated from cross-sections.

Challis volcanic group

Up to 2 km of Challis volcanic rocks (Tcv) accumulated in the Horse Prairie area between about 49 Ma and 46 Ma (Figs 1b, 2 & 5; M'Gonigle and Dalrymple, 1996). Three previous $^{40}Ar/^{39}Ar$ age determinations (M'Gonigle and Dalrymple, 1996) and five new determinations provide tight constraints on the timing of synvolcanic faulting of phase 2 and provide minimum and maximum ages for phases 1 and 3 (Fig. 5). Volcanic rocks in the Horse Prairie half graben consist largely of intermediate composition ash-flow

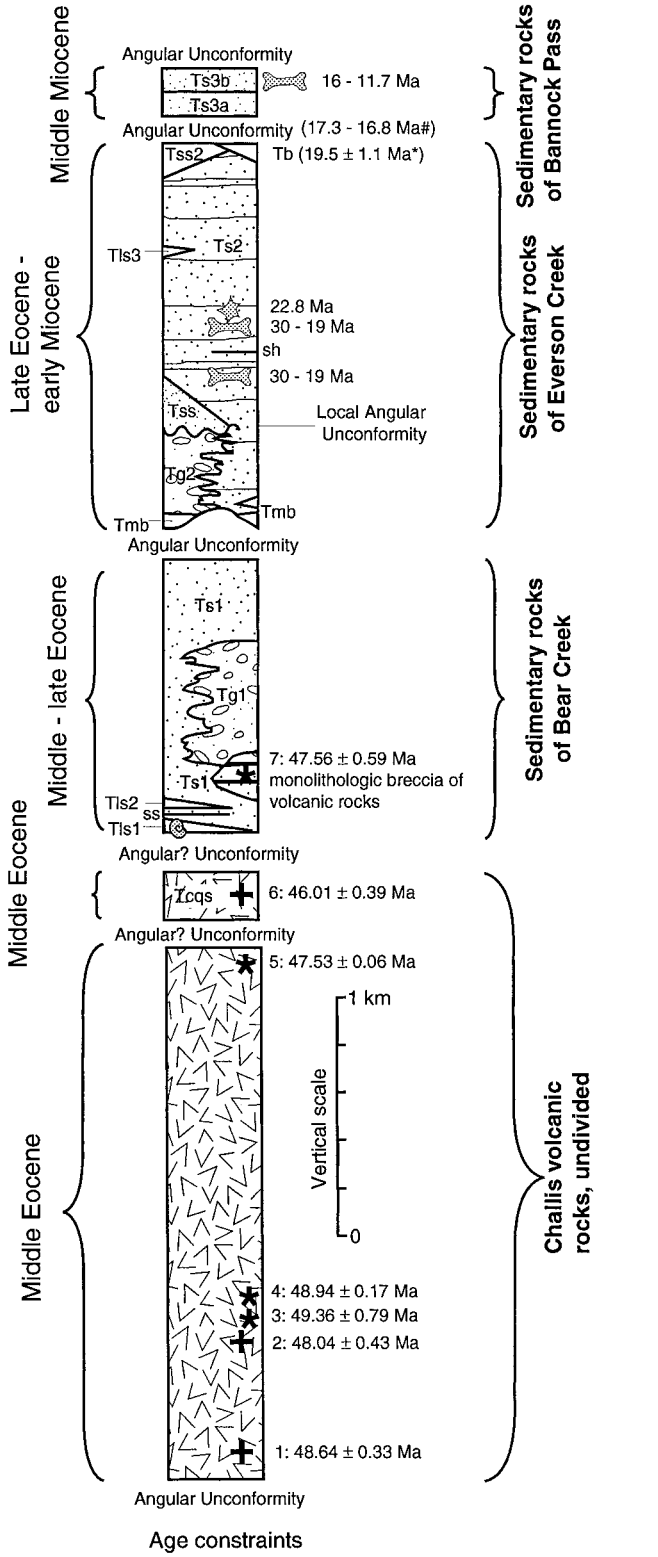

Fig. 2. Simplified stratigraphic column of Tertiary basin-fill deposits in the Horse Prairie basin showing the maximum thickness of each unit. Modified from VanDenburg (1997). Abbreviations are: quartz-sanidine bearing ash flow tuff (Tcqs); freshwater limestone (Tls1, Tls2 and Tls3); sedimentary rocks of Bear Creek (Ts1); gravel and conglomerate of Bear Creek (Tg1); monolithologic breccia deposits (Tmb); gravel and conglomerate of Everson Creek (Tg2); arkosic sandstones of Everson Creek (Tss and Tss2); sedimentary rocks of Everson Creek (Ts2); basalt (Tb); lower and upper sedimentary rocks of Bannack Pass (Ts3a and Ts3b). Argon data and sample locations are in Fig. 5. Apparent discrepancies in age determinations may be due to interlaboratory differences in monitor ages.

and ash-fall tuffs and lava flows. The volcanic stratigraphy varies dramatically across short distances with ash-flow tuffs dominating the sequence north of Bear and Trail Creeks, and lava flows dominating to the south (Fig. 5a). Although the overall thickness patterns in the volcanic rocks reflect filling of a middle Eocene ESE-trending paleovalley (Janecke, 1995b; Janecke *et al.*, in press), local thickness variations occur in association with small NE-striking synvolcanic normal faults (Figs 5a & 6a). Volcanic rocks overlie all older rocks in angular unconformity.

Tertiary basin-fill deposits

The Eocene to lower Oligocene (?) sedimentary rocks of Bear Creek (Tbc) are the oldest rift-basin deposits in the Horse Prairie half graben (Fig. 1b). They are confined to the hanging wall of the Lemhi Pass fault (LPF) in the study area (Fig. 4), but they might be present in the footwall to the east (Figs 1b & 4; M'Gonigle and Hait, 1997). Cross-section C–C′ suggests a thickness of approximately 1900 m in the subsurface (Figs 4 & 6c). A 46.01 ± 0.39 Ma quartz-sanidine ash flow tuff (Tcqs, M'Gonigle and Dalrymple, 1996; Figs 2 & 5), at the top of the Challis volcanic rocks, may be conformable with the sedimentary rocks of Bear Creek (Fig. 2), but an angular unconformity with a 19° discordance in attitude separates older Challis volcanic rocks from the sedimentary rocks of Bear Creek (Fig. 7). Some of this discordance might be due to initial dip of the older volcanic rocks. The sedimentary rocks of Bear Creek are dominated by quartzite- and volcanic-clast pebble to cobble conglomerate with interbedded sandstone, freshwater limestone, and volcanic monolithological breccia deposits (Figs 2 & 4) (VanDenburg, 1997). Molluscs in the limestone beds at the base of the sequence indicate a middle to late Eocene age (*Gyraulus proceras*; *Biomphalaria pseudoammonius*; S. Good, written communication). One of the volcanic monolithologic breccia deposits within the sedimentary package yielded a somewhat disturbed age spectrum with a preferred age of 47.56 ± 0.59 Ma (sample ♯7 in Fig. 5). The lithology of the breccia, its age [which is older than that of an underlying ash-flow tuff (sample ♯5, Fig. 5)], and its

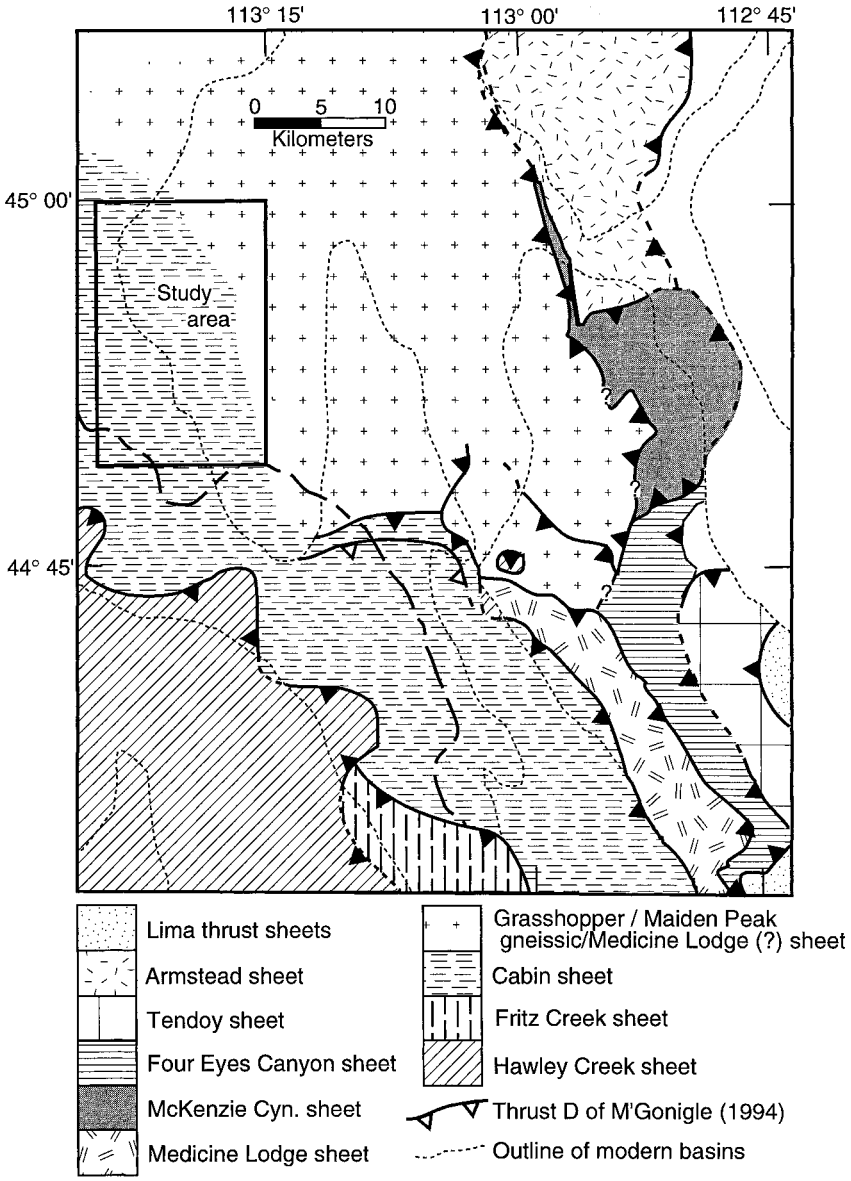

Fig. 3. Simplified map of major thrust plates of southwestern Montana. The study area lies within the Grasshopper–Maiden Peak gneissic thrust plates and within the Cabin–Medicine Lodge thrust system of Skipp (1988). Modified from M'Gonigle *et al.* (1991), Skipp (1988), Perry *et al.* (1988), McDowell (1992, 1997), VanDenburg (1997), and S. U. Janecke (unpublished mapping). Location shown in Fig. 1(a).

stratigraphic position all suggest that it is probably a rock-avalanche or rock-slide deposit derived from lava flows of the underlying Challis volcanic rocks. Deposition of the sedimentary rocks of Bear Creek is tentatively related to slip on the Muddy–Grasshopper and Agency–Yearian detachment faults (Fig. 1a).

The sedimentary rocks of Everson Creek (Tec) are the second angular-unconformity bounded sequence. This unit is exposed throughout the Horse Prairie half graben and overlies all older rocks in angular unconformity (Figs 1b & 4). These sedimentary rocks overlap the older Lemhi Pass fault, and occupy the half-graben above the west-dipping Maiden Peak fault system (Figs 1b, 4 & 6). Approximately 1.4 km of the sedimentary rocks of Everson Creek are exposed (Fig. 2). The sedimentary rocks of Everson Creek are dominated by tuffaceous siltstone, sandstone, and pebble conglomerate (Fig. 2) (VanDenburg, 1997). Locally, near the base of the section, lenses of monolithologic breccia derived from the quartz–sanidine ash-flow tuff, and quartzite-clast boulder to cobble gravels are present. Arikareean and Hemingfordian vertebrate fossils (Fields *et al.*, 1985; R. Nichols, written communication, 1995) and a 19.5 ± 1.1 Ma basalt at the top of the sedimentary rocks of Everson Creek at Red Butte (K–Ar age determination, 48% radio-

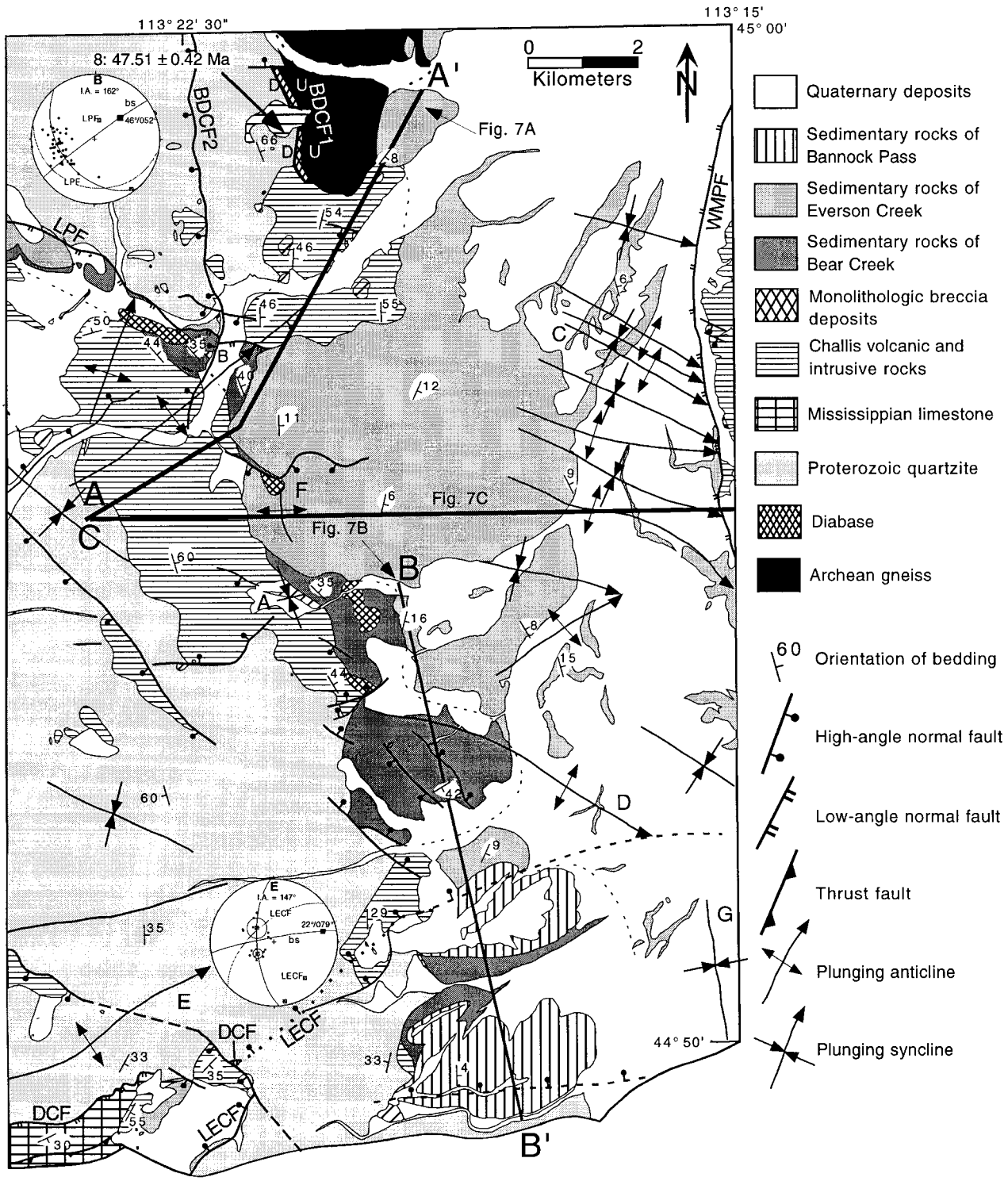

Fig. 4. Geological map of the study area. Simplified from 1:24,000 scale geologic map (VanDenburg, 1997). Continuations of contacts, faults, and folds beneath Quaternary cover are shown as solid lines for clarity. Abbreviations as in Fig. 1. Location shown in Fig. 1(b). Stereograms of poles to bedding (dots) of folds B and E show folds axes (black squares), great circles and poles to bisecting surfaces (bs, gray square), and orientation of associated normal faults (LPF or LECF). I.A. = interlimb angle.

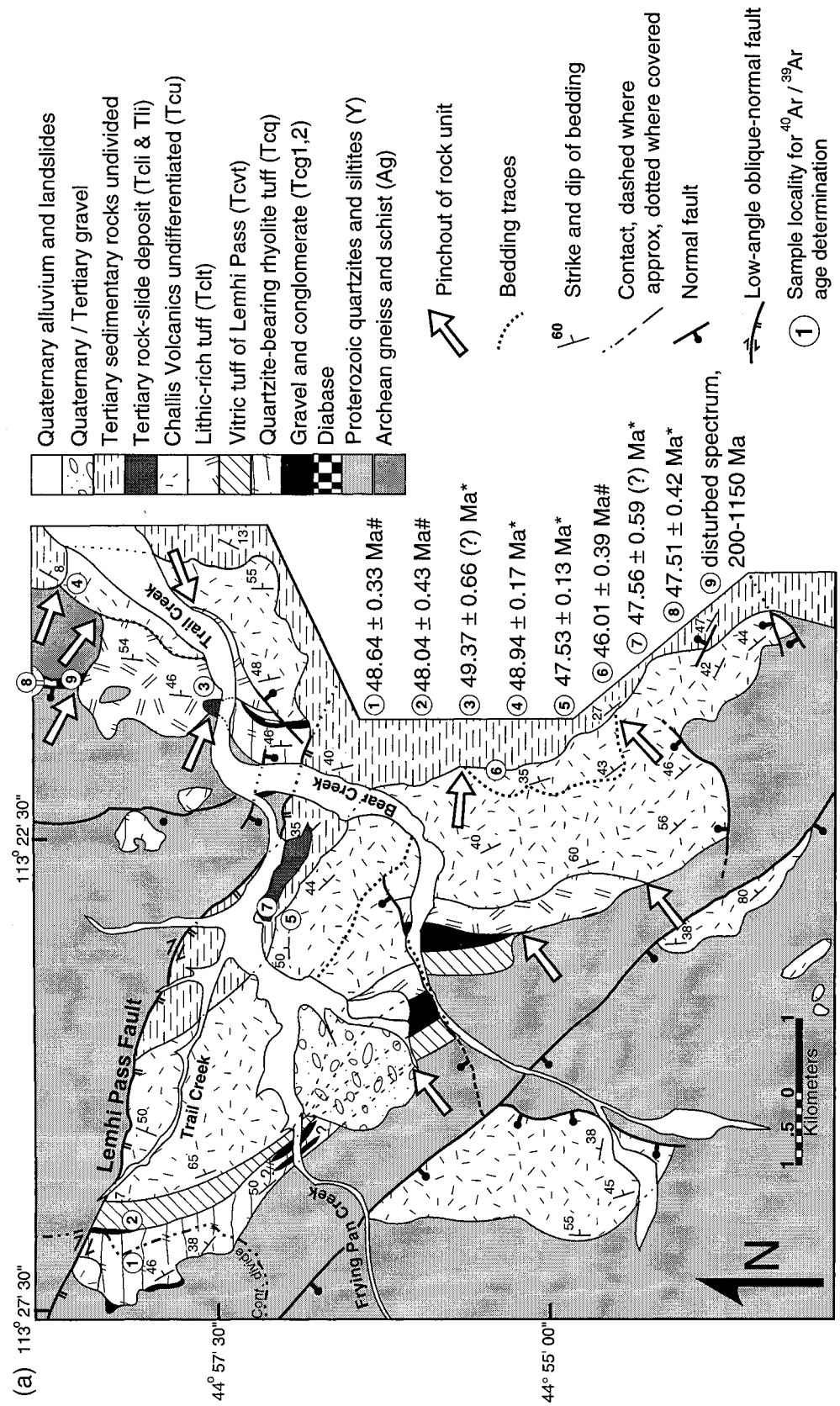

Fig. 5(a).—*Caption overleaf.*

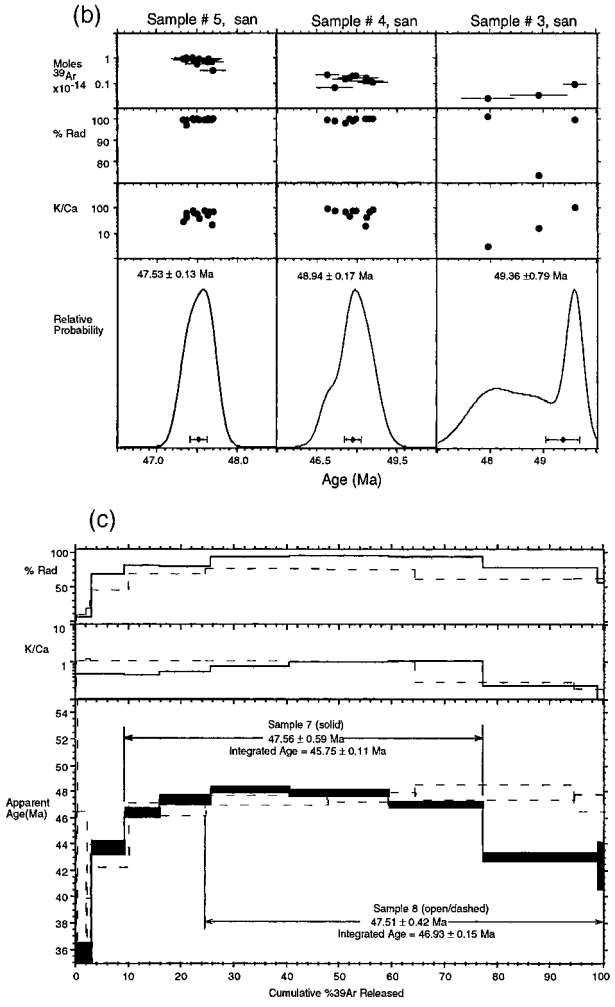

Fig. 5. Geological map of the Lemhi Pass area (a) and argon geochronology (a–c). (a) Geological map of the Lemhi Pass area showing the locations of dated igneous rocks (samples 1–9). Location shown in Fig. 1(b). ‡Age determination from M'Gonigle and Dalrymple (1996); *Age determination from this study. Compiled from VanDenburg (1997), S. U. Janecke, unpublished mapping, and Staatz (1979). Ages determined during this study are about 1% older than those of M'Gonigle and Dalrymple (1996) because different monitors were used. (b & c) $^{40}Ar/^{39}Ar$ age determinations. Samples were analyzed at the New Mexico Geochronology Research Lab using procedures detailed in McIntosh and Chamberlin (1994). All ages are relative to Fish Canyon Tuff monitor sanidine (27.84 Ma, Deino and Potts, 1990). Sample locations are shown in Figs 5(a) & 4. (b) Single-crystal laser-fusion data from sanidine. Age-probability diagrams (Deino and Potts, 1990) are accompanied by auxiliary plots showing moles of ^{39}Ar, percent radiogenic yield, and K/Ca ratios. Upper panel also shows 1 sigma analytical uncertainty for each crystal. Lower panel shows weighted mean age and 2 sigma uncertainty. Samples 5 and 4 yielded precise age determinations. Poor precision for sample 3 reflects paucity and small size of sanidine in this sample. (c) Age spectra for groundmass concentrates. Sample 8 yielded a precise plateau age (Fleck *et al.*, 1977). Sample 7 yielded a somewhat disturbed spectrum which failed to meet plateau criteria or form a well-correlated isochron; a weighted mean age was calculated for the flattest part of the age spectrum.

genic argon, McDowell, Wampler, Fritz and Sears, unpublished data) indicate that deposition of the upper 3/4 of the sedimentary rocks of Everson Creek occurred between about 30 and 20 Ma (Fig. 2).

The nearly flat-lying sedimentary rocks of Bannock Pass (Tbp) overlie the sedimentary rocks of Everson Creek with angular unconformity and yield Barstovian (middle Miocene) vertebrate fossils (Figs 1b, 2 & 4) (units Tc and Tm of M'Gonigle, 1994; Fields *et al.*, 1985; R. Nichols, written communication, 1995). These relationships imply tilting and erosion in the late early Miocene (Fig. 2). Exposures of the sedimentary rocks of Bannock Pass are largely confined to the southern Horse Prairie half graben, where a maximum thickness of 235 m is preserved (Fig. 1b; M'Gonigle, 1994; VanDenburg, 1997). The sedimentary rocks of Bannock Pass are dominated by tuffaceous siltstone and fine sandstone. The provenance of scattered conglomerate lenses within the sedimentary rocks of Bannock Pass indicate that the basin filled approximately equally from its east and west sides (M'Gonigle, 1994; VanDenburg, 1997).

The progressive decrease in dip up-section of the Tertiary volcanic and sedimentary rocks demonstrates that normal faulting was coeval with deposition of these units. The middle Eocene Challis volcanic rocks (Tcv) dip ~50° north-northeast, and are overlain unconformably by 35° NE-dipping sedimentary rocks of Bear Creek (Tbc, Figs 1b, 2 & 7), which in turn are overlain unconformably by 9° E-dipping sedimentary rocks of Everson Creek (Tec). The youngest angular unconformity is the most subtle, and separates the sedimentary rocks of Everson Creek (Tec) and older units from the 4° E-dipping sedimentary rocks of Bannock Pass (Tbp, Figs 1b, 2 & 7). All of the Tertiary rocks are gently folded, so angular discordances between units vary spatially.

EPISODIC EXTENSION

At least five geometrically and temporally distinct phases of extension affected the Horse Prairie half graben area in the late Mesozoic (?) and Cenozoic (Figs 8–10). Five large (>2 km dip slip) southwest-, northwest-, and west-dipping normal faults and at least three sets of extension-related folds deform the rocks in the study area at different stratigraphic levels. The following description of normal faults and genetically related extensional folds progresses in chronologic order from the oldest to the youngest. More detailed descriptions of the folds, including the mechanisms responsible for their formation (if known), are presented in Janecke *et al.* (1998).

Pre-middle Eocene normal (?) faults (phase 1)

The Divide Creek (DCF) and the Bloody Dick Creek faults (BDCF) are large SW-dipping normal (?) faults that predate the middle Eocene Challis Volcanic Group. Both faults may have reactivated SW-dipping

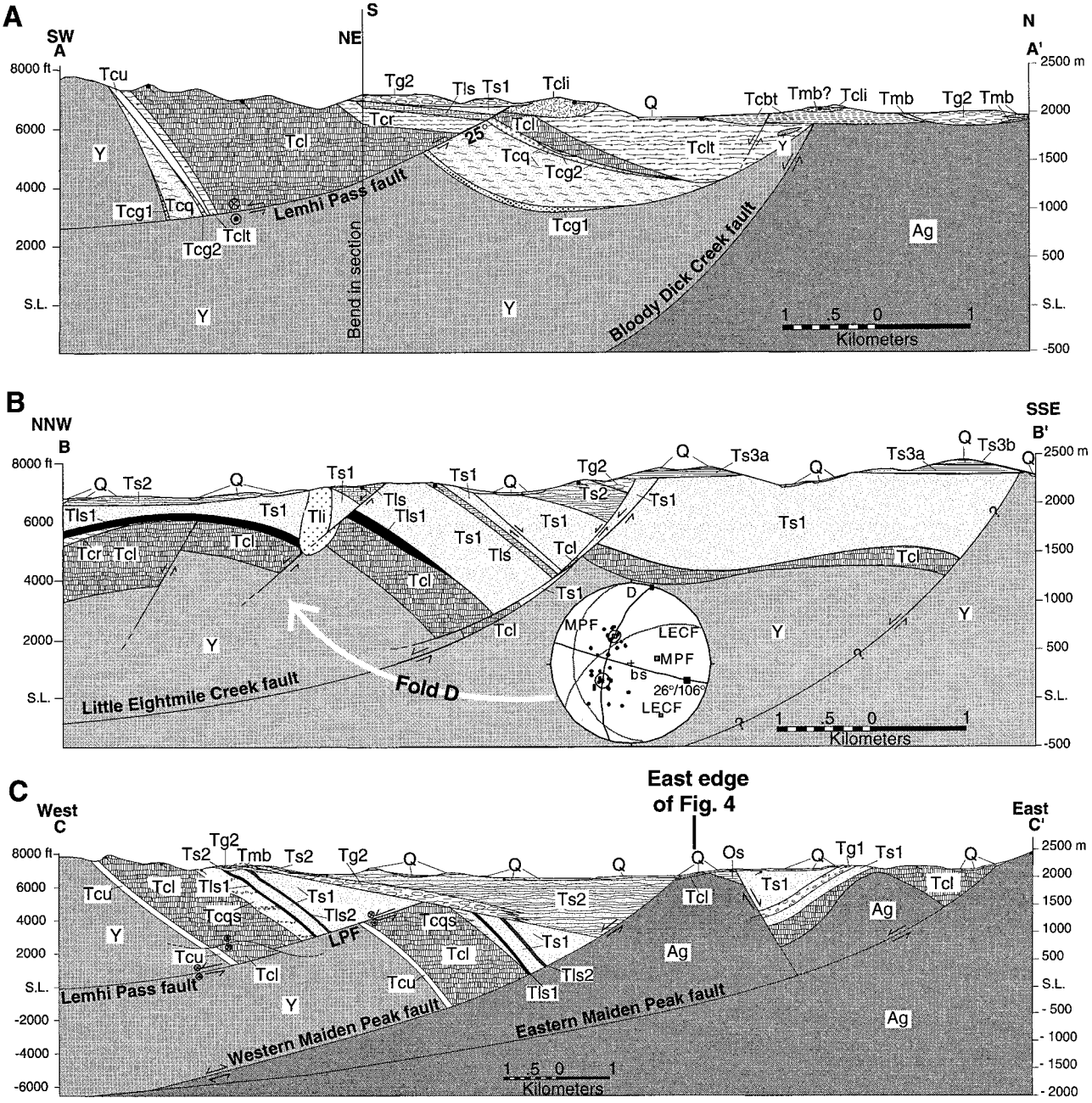

Fig. 6. (a) Cross-section A–A′. Note low-angle geometry of Lemhi Pass fault, angular discordance between unit Tcr of the Challis volcanic rocks and unit Tg2 of the sedimentary rocks of Everson Creek, and lapping relationships above the Bloody Dick Creek fault. Volcanic rocks pinch out against the margins of the Lemhi Pass paleovalley. Lines of section are shown on Fig. 4. (b) Cross-section B–B′. Note the listric geometry of the Little Eightmile Creek fault, rollover anticline D, lapping relationships with the late-Early Miocene sedimentary rocks of Bannock Pass (Ts3a, Ts3b), and changes in thickness within lava flows of the Challis volcanic rocks (Tcl) across the fault. A 75° cut-off between bedding and the Little Eightmile Creek fault was assumed to construct the cross-section. Stereogram of poles to bedding that define the axis (black square) of fold D. Orientation of bisecting surface (bs), Little Eightmile Creek fault (LECF), and the Maiden Peak fault (MPF) are also shown. (c) Cross-section C–C′. Note angular discordance between the sedimentary rocks of Bear (Ts1) and Everson (Ts2) Creek. Figure 1(c) extends this cross-section across the Medicine Lodge half graben to the east. Abbreviations as in Figs 2 and 5(a): Ordovician quartzite (Os); undifferentiated volcanic rocks (Tcu); lava flows and flow breccias, (Tcl); tuff of Curtis Ranch (Tcr); biotitic tuffs (Tcbt); undifferentiated Quaternary–Tertiary deposits (Q).

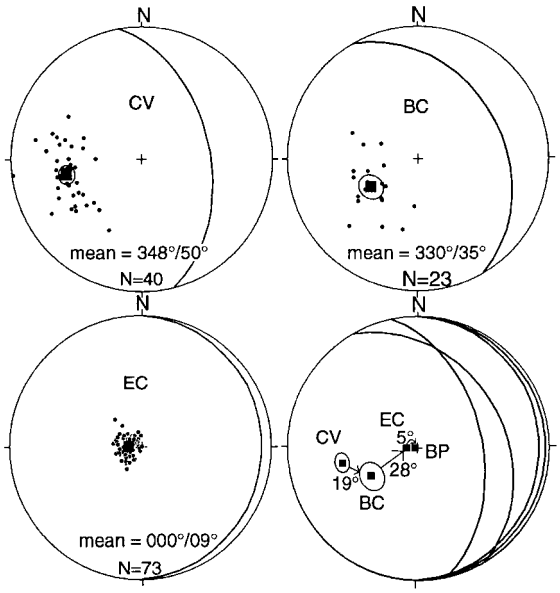

Fig. 7. Equal area stereograms of poles to bedding of Tertiary rocks in the Horse Prairie basin. Mean poles to bedding show a 19° angular discordance between Challis volcanic rocks (CV) and the sedimentary rocks of Bear Creek, a 28° angular discordance between the sedimentary rocks of Bear Creek (BC) and the sedimentary rocks of Everson Creek (EV), and 5° discordance between the sedimentary rocks of Everson Creek and the sedimentary rocks of Bannock Pass (BP). All of the deposits are folded, so the discordance at a particular location varies.

thrust faults, and could accommodate tens of kilometers of slip (Fig. 9a).

In the southwest corner of the study area, a southeast-dipping, low-angle younger-on-older fault (DCF) places Mississippian carbonates over Middle Proterozoic quartzite and siltite (Goat Mountain thrust of Staatz, 1973, 1979; VanDenburg, 1997; DCF, Figs 1b & 4). Janecke *et al.* (1998) expand on the work of Skipp (1988) to show that this fault is: (1) probably a low-angle normal fault; and (2) a portion of the regionally extensive, southwest-dipping Divide Creek fault. We cannot rule out a strike-slip (e.g. Huerta and Rodgers, 1996) or out-of-sequence thrust origin for the Divide Creek fault but most evidence supports an extensional origin (Skipp, 1988; VanDenburg, 1997).

The present 36°SE dip of the Divide Creek fault (Table 1) is partially due to subsequent tilting and folding in the hanging wall of the northwest-dipping Little Eightmile Creek fault (Fig. 4). Restoration of the Challis volcanic rocks that overlie the Divide Creek fault (Fig. 4) to horizontal, results in a strike of S13°E and a southwest dip of 28° for this segment of the Divide Creek fault (Table 1). Tens of kilometers of dip-slip separation are possible along this portion of the fault because the fault omits approximately 3 km of stratigraphy in a 'flat on flat' relationship.

The Divide Creek fault cuts rocks as young as Permian in the southern Beaverhead Mountains (Skipp, 1984), and is overlain by middle Eocene volcanic rocks in many places, permitting either a Mesozoic or Early Tertiary age (Janecke *et al.*, 1998). On a regional scale (Fig. 1a), the Divide Creek fault lies in the footwall of the late Cretaceous (?) Hawley Creek thrust, and has a trace that roughly parallels the thrust, but dips less steeply. The >100 km long Divide Creek fault probably soles into and reactivates the Hawley Creek thrust at depth.

A second pre-middle Eocene younger-on-older fault, the moderately southwest-dipping Bloody Dick Creek fault (BDCF), occurs in the northern part of the study area in the footwall of the Beaverhead Divide fault, a SW-dipping reverse fault along the Idaho–Montana border (Hansen, 1983; VanDenburg, 1997). The net normal slip on the Bloody Dick Creek fault zone is difficult to constrain because the correlation of Middle Proterozoic rocks in the footwall and hanging wall is controversial (compare Coppinger, 1974; Hansen, 1983; Ruppel *et al.*, 1993), but exposure of Archean gneisses in the footwall of the southeasternmost segment of the fault suggests that normal dip-slip separation increases to the southeast (Figs 1b & 4). The Bloody Dick Creek fault has two strands at its southern end.

Several relationships show that the older strand of the Bloody Dick Creek fault (BDCF1, Figs 1b, 4 & 6), like the Divide Creek fault, is older than the middle Eocene Challis volcanic rocks. At its southeast end, Middle Eocene lava flows and ash flow tuffs of the Challis volcanic rocks overlie both the fault and a diabase intrusion that coincides with the fault (Figs 4, 5 & 6). This diabase intrusion yielded a difficult to interpret, highly disturbed $^{40}Ar/^{39}Ar$ age spectrum with ages ranging mainly from 200 to 1150 Ma (sample ♯9, Fig. 5a). The older strand of the Bloody Dick Creek fault and the diabase are both overlain by an aphanitic mafic lava or intrusion with an $^{40}Ar/^{39}Ar$ groundmass-concentrate age of 47.51 ± 0.42 Ma (sample ♯8, Figs 4 & 5). A younger late Cenozoic normal fault (BDCF2, Fig. 4) reactivated most of the Bloody Dick Creek fault and preserves Miocene (?) sedimentary rocks in its hanging wall 1–2 km north of the study area. Further work is needed to confirm that the older strand of the Bloody Dick Creek fault is roughly coeval with the Divide Creek fault and has a similar origin.

Syn-volcanic faults (phase 2)

Cross-cutting relationships and changes in thickness across normal faults indicate that three normal faults are syntectonic with the Challis Volcanic rocks (phase 2) (Figs 4 & 9b). These faults strike northeast, dip northwest, and have dip-slip separations of the base of the Challis volcanic rocks that range from 0.9 to 1.3 km (Table 1). The northeast strike of the syn-volcanic normal faults is retained even after restoration for sub-

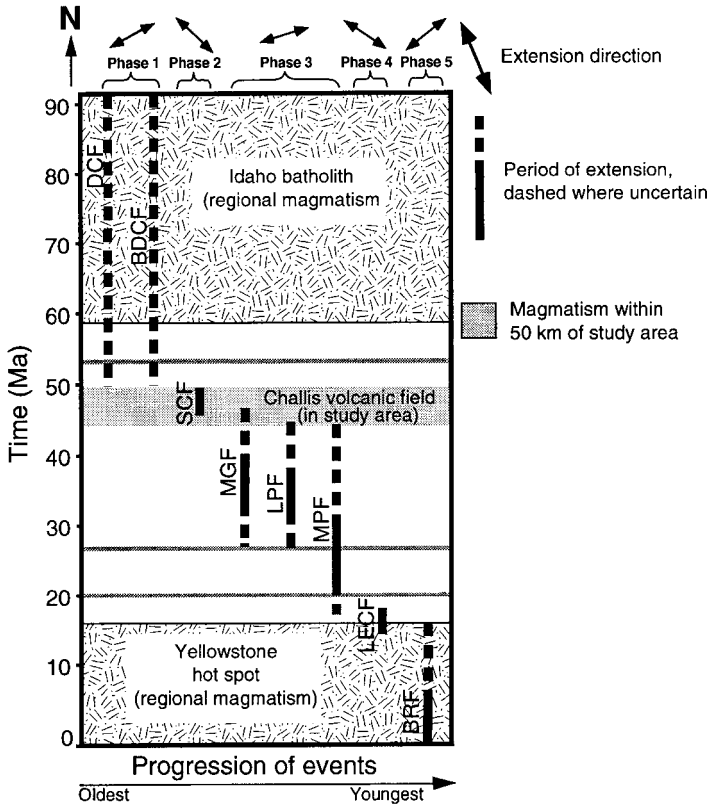

Fig. 8. Graph comparing timing of extensional phases and magmatism. Regional magmatism occurred 90–58 Ma in the Idaho batholith >125 km to the north-northwest (Desmarais, 1983; Lund and Snee, 1988) and along the Yellowstone hot spot track south of the study area (~17–0 Ma). Local magmatism was within 50 km of the study area. Extensional phases include slip on the Divide Creek (DCF), Bloody Dick Creek (BDCF), syn-Challis (SCF), Muddy-Grasshopper (MGF), Lemhi Pass (LPF), Maiden Peak (MPF), Little Eightmile Creek (LECF), and 'Basin and Range' (BRF) normal faults. Note that extension was not focused during times of local or regional magmatism.

sequent tilting. This phase of extension produced only modest amounts of northwest–southeast extension.

These northeast-striking faults were active in the middle Eocene based on cross-cutting relationships within the Challis volcanic rocks. All three structures offset the base of the Challis volcanic rocks, including the 48.04 ± 0.43 Ma tuff of Lemhi Pass (Sample ♯2 in Fig. 5; M'Gonigle and Dalrymple, 1996) and the 49.37 ± 0.66 (?) Ma lithic-rich tuff (Sample ♯3 in Fig. 5). Two of the three faults are lapped by lava flows that predate emplacement of the 47.53 ± 0.13 Ma tuff of Curtis Ranch (Sample ♯5, Figs 5 & 8). Age control (adjusted for different monitors and monitor ages) and fault displacement data suggest that the syn-volcanic normal faults had fairly high but short-lived slip rates in excess of 0.9–1.3 km/My. The age and geometry of the syn-volcanic normal faults is similar to that of other syn-volcanic normal faults in the Challis arc (McIntyre *et al.*, 1982; O'Neill and Lopez, 1985; Kiilsgaard *et al.*, 1986; Janecke, 1992, 1995a; Snider, 1995; Janecke *et al.*, 1997).

Late to post-volcanic faults (phases 3a and 3b)

The modern north–south-trending Horse Prairie half graben and most of its synrift basin-fill deposits formed during slip on the Muddy-Grasshopper fault, the master detachment fault during phase 3 (Fig. 1, Perry and M'Gonigle, 1995; Janecke *et al.*, 1996a,b), the Lemhi Pass fault (phase 3a), and the younger Maiden Peak fault system (phase 3b) (Figs 4, 9c & d). The Lemhi Pass fault, contrary to previous interpretations (Sharp and Cavender, 1962; Staatz, 1979; Hansen, 1983) dips gently (Fig. 6; VanDenburg, 1997; Blankenau and Janecke, 1997). Three-point analysis of the trace of the Lemhi Pass fault at its southeast end yields a strike of S78°E and a dip of 24° to the south southwest (Table 1). Correcting for the effects of subsequent tilting yields a strike of S58°E and a dip of 27° to the southwest (Table 1). It is difficult to quantify the component of dextral slip (if any) along the Lemhi Pass fault because slickenlines are not preserved. Dip

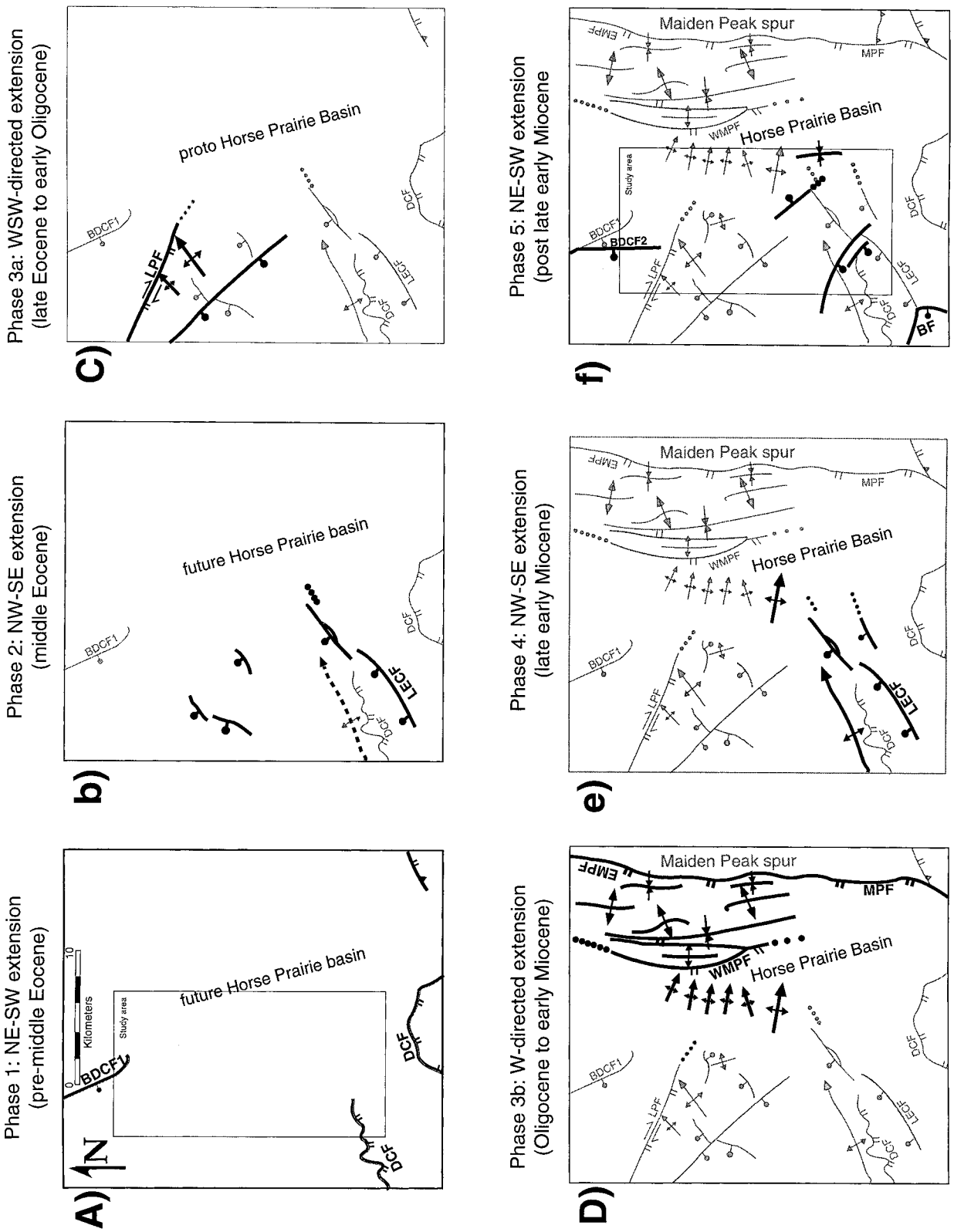

Fig. 9. Synoptic maps showing the sequential development of normal faults and extensional folds. Bolded structures formed sequentially during phases 1–5. Grayed structures are shown for reference. Abbreviations as in Fig. 8. BF = Beaverhead fault.

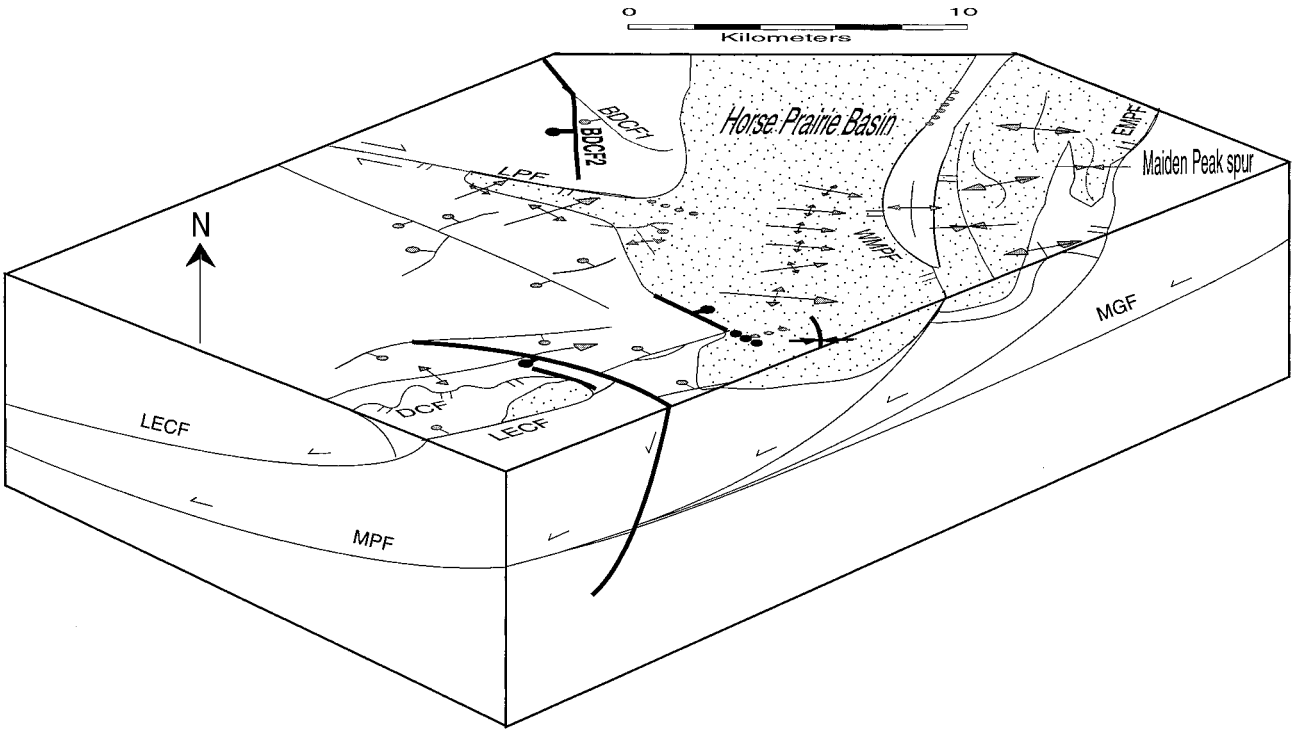

Fig. 10. Block diagram showing the present three-dimensional geometry of the study area. View is to the north. Abbreviations as in Fig. 8.

Table 1. Description of major Late Mesozoic (?) and Cenozoic normal faults in the study area

Phase of extension	Name	Age	Present geometry (Restored geometry)	Dip-slip separation	Heave/Throw	Associated extensional fold(s)†
(1) Pre-middle Eocene	Divide Creek fault	Post-Permian Pre-49.5 Ma	055°/36° (167°/28°)	10 s of km	heave≫throw	none
(1) Pre-middle Eocene	Bloody Dick Creek fault (old strand)	Post-Permian Pre-49.5 Ma	161°/51° (356°/82° (?))	unknown	unknown	none
(2) Syn-volcanic	Syn-Challis faults	Post-48.0 Ma Pre-46.0 Ma	NE-striking/ NW-dipping	0.9 km 1.3 km	0.4 km/0.8 km 0.7 km/1.1 km	none
(3a) Late to post-volcanic	Lemhi Pass fault	Post-48.6 Ma Pre-Early Miocene	102°/24° (122°/27°)	2.4 km (7.4 km)*	2.2 km/1.0 km	Anticline B and parallel folds
(3b) Late to post-volcanic	Maiden Peak fault system	Post-49.5 Ma Pre-late Early Miocene	NNW/20–35° WSW	11.7 km	9.6 km/6.7 km	fold train parallel to anticline C, anticline D, and N-trending folds between strands of the Maiden Peak fault system
(4) Basin and Range-1	Little Eightmile Creek fault	Post-Early Miocene Pre-Middle Miocene	212°/34° (?)	3.0–1.0 km	1.5 km/2.6 km– 0.5 km/0.9 km	Anticlines D and E
(5) Basin and Range-2	> Basin and Range faults	Post-Middle Miocene	NW-striking SW-dipping	1.1 km	0.6 km/0.9 km	Syncline G

*Dextral-slip separation.
†Geometric data are compiled in VanDenburg (1997) and Janecke *et al.* (1998).

separation near the easternmost exposures of the Lemhi Pass fault is 2.4 km (Figs 4 & 6).

The Lemhi Pass fault places ~35° NE-dipping gravels of the sedimentary rocks of Bear Creek (Tbc) on Challis Volcanic Group (Tcv) and Middle Proterozoic bedrock, and is overlain by ~9° east-dipping sedimentary rocks of Everson Creek (Tec, Figs 4 & 6). A gentle anticline in the hanging wall of the Lemhi Pass fault (anticline B, Fig. 4) plunges NE 46° toward the easternmost exposure of the fault. The anticline has an interlimb angle of 162°, and a fold height of approximately 750 m. It folds both Challis volcanic rocks and the sedimentary rocks of Bear Creek but not the overlying sedimentary rocks of Everson Creek.

The angular unconformity between the sedimentary rocks of Bear Creek and Everson Creek is exposed throughout the study area, but is most pronounced in the immediate hanging wall of the Lemhi Pass fault near anticline B. We interpret the 26° dip- and 30° strike-discordance between the two units (Fig. 7) as the result of tilting and folding of the sedimentary rocks of Bear Creek in the hanging wall of the Lemhi Pass fault prior to deposition of the sedimentary rocks of Everson Creek. These relationships show that the Lemhi Pass fault slipped after or during deposition of the middle to late Eocene sedimentary rocks of Bear Creek (Tbc), but slip ceased before deposition of the Oligocene to early Miocene sedimentary rocks of Everson Creek (Tec) (Fig. 8).

The Maiden Peak fault system, which bounds the Horse Prairie half graben to the east, is the second major normal fault to extend the study area during phase 3 (phase 3b) (Fig. 1b). This west-dipping fault system separates the Tertiary sedimentary and volcanic rocks of the Horse Prairie half graben in its hanging wall from Archean gneisses and Paleozoic rocks in the footwall (M'Gonigle, 1994; M'Gonigle and Hait, 1997). The Maiden Peak fault system may consist of a single fault where it bounds the southeastern Horse Prairie half graben, but bifurcates into a number of W-, E-, and SW-dipping faults to the north (M'Gonigle, 1994; M'Gonigle and Hait, 1997; Fig. 1b). Map patterns, three point analyses, an unmigrated seismic reflection profile of medium to poor quality (SL1 in Fig. 1b) and drilling data all suggest low to moderate dips (20–35°) along strands of the Maiden Peak fault system (M'Gonigle, 1994; E. Brenner-Younggren, cited in M'Gonigle and Hait, 1997; M'Gonigle and Hait, 1997; VanDenburg, 1997). A lack of substantial post-Early Miocene extension and tilting in the vicinity of the Maiden Peak fault suggests that its current gentle dip is representative of its attitude during the latest phases of slip.

A total dip-slip separation of 11.7 km, with 9.6 km of heave and 6.7 km of throw, is estimated across the three splays of the Maiden Peak fault system along an east–west transect at 45° 55′ N latitude (Fig. 6 & Table 1). The eastern and western splays of the fault system account for 5.2 km and 4.8 km of the total 11.7 km of dip-slip separation, respectively. North-trending synclines and anticlines fold Tertiary sedimentary rocks and volcanic rocks and underlying bedrock between strands of the Maiden Peak fault system (M'Gonigle and Hait, 1997). The folded Tertiary sedimentary rocks display growth relationships and, therefore, formed during slip on the Maiden Peak fault system.

Cross-cutting relationships loosely bracket the timing of extension on the Maiden Peak fault system between middle Eocene and early Miocene time (Fig. 8). The fault system cuts Challis volcanic rocks, the sedimentary rocks of Everson Creek (including the 19.5 Ma basalt flow), and may cut the middle Miocene sedimentary rocks of Bannock Pass (M'Gonigle, 1994). The latest slip ended before deposition of younger gravel deposits (QTg; M'Gonigle, 1994; M'Gonigle and Hait, 1997). Growth relationships and facies patterns within the sedimentary rocks of Everson Creek show that the fault was well-established by middle Oligocene time, but that slip may have initiated earlier (VanDenburg, 1997).

In the hanging wall of the western splay of the Maiden Peak fault system, 11 anticlines and synclines plunge gently east-southeast toward the fault (Fig. 4, Fold C). Subtle strike changes define the folds, which also appear on a north–south seismic line through the basin (SL2, Fig. 1b). The folds have an average spacing of 0.7 km, die out to the west-northwest and deform the same units cut by the Maiden Peak fault. These relationships suggest that the fold train is related to the Maiden Peak fault, but the precise mechanism of deformation is uncertain (Janecke *et al.*, 1998). Irrespective of their origin, these extensional folds are evidence for three-dimensional strain during slip on the Maiden Peak fault system.

Basin and Range faults (phases 4 and 5)

Whereas Paleogene normal faulting dominated the extensional history of the Horse Prairie half graben, two phases of Late Cenozoic extension also deformed the area. The first of these phases was accommodated along a reactivated synvolcanic normal fault from phase 2, the northeast-striking Little Eightmile Creek fault (phase 4) (Figs 4 & 9e). The presence of a northeast-plunging longitudinal fault-bend anticline in the hanging wall of the Little Eightmile Creek fault (Fold E, Figs 4 & 6) indicates a listric geometry in the subsurface. Cross-section B–B′ shows 1.0 km of dip-slip separation, 0.5 km of heave and 0.9 km of throw on the basal Tertiary contact across the Little Eightmile Creek fault (Figs 4 & 6b; Table 1). The amount of slip increases to the southwest, however, where the fault shows up to 3.0 km of dip-slip separation (Table 1). Most of the dip-slip separation accumulated during phase 4.

The age of the Little Eightmile Creek fault is well constrained at its northeast end, where the fault cuts the SE-dipping, Oligocene to early Miocene sedimentary rocks of Everson Creek in the hanging wall, and is overlain by 4° E-dipping, middle Miocene sedimentary rocks of Bannock Pass (Figs 4 & 6). At this location, the sedimentary rocks of Everson Creek are folded into a southeast-plunging anticline (Fold D, Figs 4 & 6b), whereas the overlying sedimentary rocks of Bannock Pass are merely tilted. The anticline, which has a fold-height of >1 km and converges on the projected trace of the Little Eightmile Creek fault at its eastern end, probably formed as a rollover into both the NW-dipping Little Eightmile Creek fault and the W-dipping western strand of the Maiden Peak fault system (Fig. 9).

The second phase of late Cenozoic extension in the Horse Prairie half graben (phase 5) occurs on several SW- and NE-dipping normal faults in the southern half of the study area (Figs 4 & 9f). These NW-striking Basin and Range faults have small displacements in the study area (typically <1 km dip-slip separation), and lack associated syntectonic sedimentary rocks. This phase of extension did not extend the study area significantly, but major active NW-striking Basin and Range normal faults occur southwest and northeast of the study area (Scott *et al.*, 1985; Stickney and Bartholomew, 1987; Crone and Haller, 1991; BF, BTF, RRF in Fig. 1 a & b). Extensional folding occurred during phase 5 along a subtle NNW-trending syncline that roughly coincides with the axis of the modern Horse Prairie half graben (Fold G, Fig. 4). This syncline is clearly a young structure because it folds the middle Miocene sedimentary rocks of Bannock Pass that overlap normal faults and folds formed during phase 4.

STRUCTURAL IMPLICATIONS

Summary of structural history and its regional context

The Horse Prairie area had a long and complex extensional history that resulted in a time-integrated three-dimensional strain. Crustal thinning began >50 Ma, prior to Challis volcanism, and continued in phases to the present (Figs 8–10). The SW-dipping Divide Creek and Bloody Dick Creek faults are the oldest normal (?) faults and probably reflect a phase of Mesozoic or early Cenozoic northeast–southwest extension. These structures clearly predate other normal faults in the study area. This phase may have initiated in the late Cretaceous during the Sevier orogeny or might immediately predate Challis volcanism if the faults are broadly correlative with SW-dipping shear zones in the Pioneer core complex of central Idaho (Silverberg, 1990). Further work is needed to constrain the age of this deformation.

The first tightly constrained phase of Cenozoic extension occurred on NW-dipping, syn-volcanic faults. The magnitude of this short-lived phase of northwest–southeast extension may in part be masked by middle Eocene paleotopography, but was much less than the magnitude of extension associated with phase 1 or phase 3 (Table 1).

In late middle Eocene to early Miocene time, after the decline of Challis volcanism, the Horse Prairie half graben experienced a second phase of northeast–southwest extension on the Muddy–Grasshopper, Maiden Peak, and Lemhi Pass fault systems (phases 3a and 3b). This protracted event extended the crust in a direction similar to the pre-volcanic faults (phase 1), and may reflect continued gravitational collapse subsequent to a brief interruption during Challis volcanism. The Horse Prairie–Medicine Lodge and Grasshopper half graben were originally bounded on the east by the WSW-dipping Muddy–Grasshopper detachment fault, and were later dissected by the Maiden Peak and Lemhi Pass fault systems (M'Gonigle and Dalrymple, 1993; this study). The Muddy–Grasshopper fault, which lies at the crest of the Tendoy Range, 20 km east of the Horse Prairie half graben, was the breakaway fault separating extended hanging wall to the west from intact footwall to the east (Perry and M'Gonigle, 1995; Janecke *et al.*, 1996a,b). The Salmon rift basin, to the west of the Horse Prairie basin, lies in the hanging walls of two structurally higher detachment faults (AYF and SBF, Fig. 1a), but has a tectonic evolution that is broadly parallel to that of the coeval basins in its footwall (Blankenau and Janecke, 1997; Blankenau, in press). The third phase of normal faulting was responsible for the bulk of the extensional strain in the study area, and preserved the majority of the Tertiary basin-fill deposits.

Another period of northwest–southeast extension interrupted the persistent northeast–southwest extension direction in the late early Miocene (phase 4). NW-striking faults, which are seismically active in the region, represent the fifth and final phase of extension in the study area. This phase follows the persistent northeast–southwest extension direction, but is probably too far removed in time from Sevier-age crustal shortening to reflect continued gravitational collapse. Active mantle upwelling may be the ultimate cause of the youngest deformation (Liu and Shen, 1998).

Every one of the extensional events in the Horse Prairie area is a regional feature, and some (phases 3 and 5, and perhaps 1) affected much of the U.S. cordillera. Phase 1 affected several mountain ranges adjacent to the Horse Prairie area (Fig. 1a) and may be related to widespread late Cretaceous gravitational collapse of the Sevier orogenic belt during convergence (Hodges and Walker, 1992) or to an enigmatic ~50

Ma event (Silverberg, 1990) in central Idaho. Synvolcanic faults of phase 2 pervade the Challis arc in central Idaho during the middle Eocene (see fig. 1 of Janecke *et al.*, 1997 and references therein). Normal faults of phase 3 developed in a narrow (100 ± 25 km) north-trending rift zone that stretched south from British Columbia to the northern Great Basin (Axen *et al.*, 1993; Janecke, 1994), whereas NE-striking normal faults of phase 3 have only been documented northeast of the study area (Fritz and Sears, 1993; Sears *et al.*, 1995, 1998). Basin and Range normal faults of phase 5 occur throughout the Rocky Mountain, northern and central Basin and Range province (Wernicke, 1992).

In the absence of independent evidence (e.g. Lemhi Pass fault), we assume that the extension direction for each phase is nearly perpendicular to the strike of the active normal fault. This assumption is based on the younger-on-older geometry of all the faults, thick accumulations of synrift basin-fill deposits preserved in the hanging walls of many faults, and kinematic evidence for dip slip on correlative normal faults in adjacent areas (Janecke, 1992).

Origin of changing extension directions

Northeast–southwest to ENE–WSW extension characterized much of the late Cretaceous (?) to Cenozoic evolution of the area (phases 1, 3, 5), and was interrupted briefly in the middle Eocene (phase 2) and late-Early Miocene (phase 4) by minor phases of NW–SE extension (Figs 8–10). Four changes in extension direction occurred, each recording a near 90° change in the dominant extension direction (Figs 8–10). The normal faults that accommodated the bulk of the extension (Divide Creek, Bloody Dick Creek, Muddy–Grasshopper, and Maiden Peak faults) generally parallel contractional structures in the region, and may have reactivated pre-existing Mesozoic to early Tertiary thrusts and Middle Proterozoic normal faults in the subsurface.

The many changes in extension direction in the study area can be interpreted as a protracted history of roughly NE–SW to ENE–WSW gravitational collapse of the Sevier fold and thrust belt, interrupted by two short intervals of northwest–southeast extension in middle Eocene and late-early Miocene time. The first of five sets of faults in the Horse Prairie area, the Divide Creek and older strand of the Bloody Dick Creek fault, appear to merge with, and reactivate thrust faults in the subsurface. In the northern Lemhi Range, normal faults of the same age (pre-middle Eocene) and geometry as the Divide Creek and the older strand of the Bloody Dick Creek faults, reactivate thrust faults at the present level of exposure (Tysdal, 1996a,b; Tysdal and Moye, 1996), in agreement with a gravitational collapse model. In middle Eocene times, northeast–southwest extension of the NNW-trending fold and thrust belt was briefly interrupted by an phase of northwest–southeast syn-volcanic extension of the Challis volcanic arc (phase 2). Magmatism and rapid northwest–southeast convergence between oceanic plates and the North American plate at this time may have contributed to the 90° flip of extension directions (Janecke, 1992). ENE–WSW gravitational collapse re-established itself near the end of Challis volcanism (~45 Ma) (phase 3a) and continued until another brief interruption in the late-Early Miocene (phase 4). Northwest–southeast late-Early Miocene extension across the Little Eightmile Creek fault (phase 4) may reflect the initiation of Basin and Range style extension in the study area, but the mechanism responsible for this short-lived phase, with its anomalous fault patterns, is enigmatic (Fritz and Sears, 1993; Sears, 1995). Northeast–southwest extension again re-established itself after the late-Early Miocene, and continues to the present in this region (Stickney and Bartholomew, 1987; Piety *et al.*, 1992).

The origin of the near 90° shifts in extension direction may in part be due to pre-existing faults with northeast and northwest strikes. Several studies in the region suggest that the orientation of pre-Cenozoic structures strongly influenced the orientation of subsequent faults (Schmidt *et al.*, 1984, 1993; McDowell, 1992; Kellogg *et al.*, 1995; Janecke *et al.*, 1996a). In particular, NE- and NW-striking faults have been recurrently active since the early Proterozoic (Harlan *et al.*, 1996; Schmidt, 1996). Inheritance may have played a role in the development of the Divide Creek, Bloody Dick Creek, western strand of the Maiden Peak, and Little Eightmile Creek faults.

Magmatism has played a minor role in the extensional history of the Horse Prairie area. The timing of extension there was independent of both regional and local magmatic events during all but phase 2 (Fig. 8). The geometry and duration of faulting during phase 3 suggest that gravitational collapse was the ultimate cause of extension, but middle Eocene Challis volcanism may have acted as a thermal trigger for this event.

Three-dimensional strain in the study area

Alternating nearly orthogonal extension directions and three-dimensional strain during individual phases of extension contributed to the overall three-dimensional structure of the study area. Phases 3a and 3b exhibit the greatest degree of non-plane strain of all the phases of deformation (Figs 9 c & d) based on the variable orientations of normal faults (N- and NNW-striking) and folds (NE-, ESE- and N-trending).

Folds are responsible for much of the three-dimensional strain during individual phases of extension. Extensional folds occur at three distinct stratigraphic levels in association with late to post-volcanic normal faults (phases 3a and 3b), and two phases of Basin and Range extension (phases 4 and 5). Folds are typically gentle, occur in fold trains of similar age and

orientation, and have spacing ranging from 0.5 to 5.6 km, sub-vertical bisecting surfaces, and fold heights ranging from tens of meters up to 1 km (Janecke *et al*., 1998). Most of the extensional folds are oblique to, and plunge gently (20°–30°) towards, the associated normal fault, and indicate three-dimensional strain during individual phases of deformation.

Late to post-Challis and younger extension calculated using the line length of the basal Tertiary unconformity along an east–west transect through the Lemhi Pass and Maiden Peak fault systems (Fig. 6c) yields a net extension of approximately 63% (Fig. 1d). In contrast, only 20% extension was calculated for a NNW–SSE transect through the southern half of the study area (Fig. 6b), and 32% extension for a NNE–SSW transect through the northwestern corner of the study area for an average of 26% north–south extension (Figs 1d, 4 & 6a). Extension across the Divide Creek and Bloody Dick Creek faults is difficult to quantify due to poor stratigraphic control, but would greatly increase the northeast–southwest component of extension.

DISCUSSION

Many workers have described three-dimensional strain in extensional settings in recent years (Gibbs, 1987; Best, 1988; Ebinger, 1989; Bartley *et al*., 1990; Yin and Dunn, 1992; Janecke, 1992; Bohannon *et al*., 1993; Anderson and Barnhard, 1993a,b; Fritz and Sears, 1993; Schlische, 1993, 1995; Mancktelow and Pavlis, 1994; Evans and Oaks, 1996; Serpa and Pavlis, 1996; Dorsey and Robert, 1996; Fillmore and Walker, 1996; MacCready *et al*., 1997; Faulds and Varga, 1998) but usually ascribe it to 1 or 2 tectonic events. When multiple episodes of extension are documented (Zoback *et al*., 1981; Taylor *et al*., 1989; Axen *et al*., 1993; Constenius, 1996; Wells, 1997; Camilleri and Chamberlain, 1997) the extension direction is typically constant. Nonetheless, the evidence for three or more events with major changes in extension direction is growing, especially in the Great Basin (Link, 1982; Platt and Royse, 1989; Fryxell, 1991; Smith, 1997; Janecke and Evans, in press) and the Rocky Mountain Basin and Range province (McIntyre *et al*., 1982; O'Neill and Pavlis, 1988; Silverberg, 1990; Janecke, 1992; Blankenau and Janecke, 1997; Blankenau, in press). Although the Horse Prairie area may be somewhat more complex than is typical, it nonetheless shares many characteristics with other rift zones and illustrates the types of relationships that may develop during a protracted extensional history. Based on our experience in the Horse Prairie area (where we expected to find only two generations of normal faults and found five) we predict that future detailed work in other rift zones will reveal similar three-dimensional complexities. The North Sea area, with its multidirectional rift basins and long history of extension (Ziegler and van Hoorn, 1989) might have such a structural evolution.

It is critical to recognize that three-dimensional strain is both common and significant in continental rift zones. The failure to do so can result in major errors of interpretation. For example, estimates of pre-extensional crustal thickness are likely to be incorrect when the third dimension is ignored and the tectonic evolution of an area may be misinterpreted (Mancktelow and Pavlis, 1994).

A second consequence of the multiple generations of variously oriented normal faults in a rift zone are multiple superposed depocenters with unique distributions and geometries. In the geological record these are expressed as multiple angular unconformity-bounded packages of basin fill, each indicating a unique arrangement of depocenters and fault-bounded highlands. The result is a compound basin with a complex three-dimensional geometry. The deepest part of the Horse Prairie half graben, for example, is bounded on the northeast, east and southeast sides by basinward-dipping normal faults that young in a clockwise direction (Figs 9 & 10). As a result this basin contains deposits that thin abruptly along strike, down dip, and across normal faults of various ages and orientations (VanDenburg, 1997). Three-dimensional facies patterns are even more strongly developed in the southeast part of the adjacent Salmon basin (Blankenau and Janecke, 1997). In areas that experience more than one phase of extension, structures controlling the present topographic basin do not necessarily control the distribution and thickness of basin-fill deposits. Faults and folds at a high angle to the overall structural grain of a rift zone may define intrabasinal highlands that could be misinterpreted as basin-bounding structures.

Two-dimensional treatments of three-dimensional extensional terranes will introduce many inaccuracies. Parallel cross-sections differ significantly and no single section can accurately depict the overall geometry of an area. A failure to recognize the movement of material in and out of the plane of cross-section will compromise balanced cross-sections, and invalidate structural interpretations. New techniques may be required to analyze and depict such structurally complex regions. In our study, for example, section C–C′ lies perpendicular to the overall structural grain of the physiographic Horse Prairie basin yet fails to capture any NE-striking normal faults from phase 1 or 3 (Fig. 6c). The common practice of strip-mapping to constrain regional cross-sections in poorly known orogens could therefore result in major errors of interpretation when the deformation is highly three-dimensional.

CONCLUSIONS

The Cenozoic extensional history of the Horse Prairie half graben is characterized by at least five temporally distinct phases of normal faulting, and at least three generations of folding related to extension. Folds are typically at a high angle to the associated normal fault, and produce three-dimensional strain within individual phases of extension. In addition, faults have alternating northeast and northwest strikes, which produced a time-integrated three-dimensional strain. The dominant mechanism driving extension appears to have been collapse of the Sevier fold and thrust belt, possibly beginning in late Cretaceous times and persisting at least to the early Miocene.

Acknowledgements—We would like to thank Enserch Exploration for providing seismic reflection profiles from the Horse Prairie basin, John M'Gonigle, James Blankenau, James Sears, and Rob McDowell for helpful discussions and sharing data, James Evans and John M'Gonigle for reviewing an earlier version of the manuscript, and all the property owners in the Horse Prairie for permission to map on their land. Ralph Nichols kindly provided locality and age information concerning vertebrates collected within the basin-fill deposits. Financial support by the National Science Foundation (grant EAR 93-17395, Janecke) and the Tobacco Root Geological Society (VanDenburg) is greatly appreciated. We are grateful to the personnel of the Forest Service and the Bureau of Land Management for loaning us aerial photographs. The manuscript benefited from thorough and constructive reviews by Stuart Hardy, Terry Pavlis, and associate editor Donald Fisher.

REFERENCES

Anderson, R. E. and Barnhard, T. P. (1993a) Aspects of three-dimensional strain at the margin of the extensional orogen, Virgin River depression area, Nevada, Utah, and Arizona. *Geological Society of America Bulletin* **105,** 1019–1052.

Anderson, R. E. and Barnhard, T. P. (1993b) Heterogeneous Neogene strain and its bearing on horizontal extension and horizontal and vertical contraction at the margin of the extensional orogen, Mormon Mountains area, Nevada and Utah *U.S. Geological Survey Bulletin* **2011**.

Axen, G. J., Taylor, W. J. and Bartley, J. M. (1993) Space-time patterns and tectonic controls of Tertiary extension and magmatism in the Great Basin of the western United States. *Geological Society of America Bulletin* **105,** 56–76.

Bartley, J. M., Fletcher, J. M. and Glazner, A. F. (1990) Tertiary extension and contraction of lower-plate rocks in the central Mojave metamorphic core complex, southern California. *Tectonics* **9,** 521–534.

Best, M. G. (1988) Early Miocene change in direction of least principal stress, southwestern United States: Conflicting inferences from dikes and metamorphic core-detachment fault terranes. *Tectonics* **7,** 249–259.

Blankenau, J. J. in press. Tertiary tectonic evolution of the southeast Salmon basin, east-central Idaho. M.Sc. thesis, Utah State University.

Blankenau, J. J. and Janecke, S. U. (1997) Three-dimensional structure of a Paleogene rift basin and its effects on synextensional sedimentation, Salmon basin ID. *Geological Society of America Abstracts with Programs* **29,** 221.

Bohannon, R. G., Grow, J. A., Miller, J. J. and Blank, R. H. J. (1993) Seismic stratigraphy and tectonic development of the Virgin River depression and associated basins, southeastern Nevada and northwestern Arizona. *Geological Society of America Bulletin* **105,** 501–520.

Camilleri, P. A. and Chamberlain, K. R. (1997) Mesozoic tectonics and metamorphism in the Pequop Mountains and Wood Hills region, northeast Nevada: Implications for the architecture and evolution of the Sevier orogen. *Geology* **109,** 107–126.

Constenius, K. N. (1996) Late Paleogene extensional collapse of the Cordilleran foreland fold and thrust belt. *Geological Society of America Bulletin* **108,** 20–39.

Coppinger, W. (1974) Stratigraphic and structural study of Belt Supergroup and associated rocks in a portion of the Beaverhead Mountains, southwest Montana, and east-central Idaho. Ph.D. dissertation, Miami University.

Crone, A. J. and Haller, K. M. (1991) Segmentation and coseismic behavior of Basin and Range normal faults: Examples from east-central Idaho and southwestern Montana, U.S.A.. *Journal of Structural Geology* **13,** 151–164.

Deino, A. L. and Potts, R. (1990) Single-crystal $^{40}Ar/^{39}Ar$ dating of the Olorgesailie Formation, southern Kenya Rift. *Journal of Geophysical Research* **95,** 8453–8470.

Desmarais, N. R. (1983) Geology and geochronology of the Chief Joseph plutonic-metamorphic complex, Idaho–Montana. Ph.D. dissertation, University of Washington.

Dorsey, R. J. and Roberts, P. (1996) Evolution of the Miocene north Whipple Basin in the Aubrey Hills, western Arizona, upper plate of the Whipple detachment fault. In *Reconstructing the History of Basin and Range Extension Using Sedimentology and Stratigraphy*, ed. K. K. Beratan, pp. 127–146. Geological Society of America Special Paper, **303**.

Dubois, D. P. (1982) Tectonic framework of basement thrust terrane, northern Tendoy Range, southwestern Montana. In *Geologic Studies of the Cordilleran Thrust Belt*, ed. R. B. Powers, Vol. 1, pp. 145–158. Rocky Mountain Association of Geologists.

Ebinger, C. J. (1989) Geometric and kinematic development of border faults and accommodation zones, Kivu-Rusizi rift, Africa. *Tectonics* **8,** 117–133.

Evans, J. C. and Janecke, S. U. (1998) Preliminary analysis of the folded and faulted Miocene-Pliocene Salt Lake Formation in the Deep Creek half-graben, SE Idaho. *Geological Society of America Abstracts with Programs* **29,** 9.

Evans, J. P. and Oaks, R. Q., Jr (1996) Three-dimensional variations in extensional fault shape and basin form: The Cache Valley basin, eastern Basin and Range province, United States. *Geological Society of America Bulletin* **108,** 1580–1593.

Faulds, J. E. and Varga, R. J. (1998) The role of accommodation zones and transfer zones in the regional segmentation of extended terranes. In *Geological Society of America Special Paper*, eds J. H. Stewart and J. E. Faulds, **323,** 1–45.

Fields, R. W., Tabrum, A. R., Rasmussen, D. L. and Nichols, R. (1985) Cenozoic rocks of the intermontane basins of western Montana and eastern Idaho. In *Cenozoic Paleogeography of the West Central U.S.*, eds R. M. Flores and S. S. Kaplan, pp. 9–36. Denver, Colorado, Rocky Mountain Section, Society of Economic Paleontologists and Mineralogists.

Fillmore, R. P. and Walker, J. D. 1996. Evolution of a supradetachment extensional basin: The Lower Miocene Pickhandle Basin, central Mojave Desert, California. In *Reconstructing the History of Basin and Range Extension Using Sedimentology and Stratigraphy,* ed. K. K. Beratan. Geological Society of America Special Paper **303,** pp. 107–126.

Fleck, R. J., Sutter, J. F. and Elliot, D. H. (1977) Interpretation of discordant $^{40}Ar/^{39}Ar$ age-spectra of Mesozoic tholeiites from Antarctica. *Geochimica Cosmochimical Acta* **41,** 15–32.

Fritz, W. J. and Sears, J. W. (1993) Tectonics of the Yellowstone hot spot wake in southwestern Montana. *Geology* **21,** 427–430.

Fryxell, J. E. (1991) Tertiary tectonic denudation of an igneous and metamorphic complex, west-central grant range, Nye county Nevada. In *Geology and Ore Deposits of the Great Basin; Symposium Proceedings*, eds G. L. Raines, R. E. Lisle, R. W. Schafer and W. H. Wilkinson, pp. 87–92.

Gans, P. B., Mahood, G. A. and Schermer, E. (1989) Synextensional magmatism in the Basin and Range Province; a case study from the eastern Great Basin *Geological Society of America Special Paper* **233**.

Gibbs, A. (1987) Development of extension and mixed-mode sedimentary basins. In *Continental Extensional Tectonics*, eds M. P. Coward, J. F. Dewey and P. L. Hancock, pp. 19–33. Geological Society Special Publication, **28**.

Gibbs, A. D. (1984) Structural evolution of extensional basin margins. *Journal of the Geological Society of London* **141,** 609–620.

Hanneman, D. L. (1989) Cenozoic basin evolution in a part of southwest Montana. Ph.D. dissertation, University of Montana.

Hansen, P. M. (1983) Structure and stratigraphy of the Lemhi Pass area, Beaverhead Range, southwest Montana and east-central Idaho. M.Sc. thesis, Pennsylvania State University.

Harlan, S. S., Geissman, J. W., Lageson, D. R. and Snee, L. W. (1988) Paleomagnetic and isotopic dating of thrust-belt deformation along the eastern edge of the Helena salient, northern Crazy Mountains Basin, Montana. *Geological Society of America Bulletin* **100,** 492–499.

Harlan, S. S., Schmidt, C. J. and Geissman, J. W. (1996) Nature and timing of recurrent movement on NW-trending faults in SW Montana: Middle (?) Proterozoic to Neogene history. *Geological Society of America Abstracts with Programs* **28,** 509.

Hodges, K. V. and Walker, J. D. (1992) Extension in the Cretaceous Sevier orogen, North American Cordillera. *Geological Society of America Bulletin* **104,** 560–569.

Huerta, A. D. and Rodgers, D. W. (1996) Kinematic and dynamic analysis of a low-angle strike-slip fault: The Lake Creek fault of south central Idaho. *Journal of Structural Geology* **18,** 585–593.

Janecke, S. U. (1992) Kinematics and timing of three superposed extensional systems, east-central Idaho: Evidence for an Eocene tectonic transition. *Tectonics* **11,** 1121–1138.

Janecke, S. U. (1994) Sedimentation and paleogeography of an Eocene to Oligocene rift zone, Idaho and Montana. *Geological Society of America Bulletin* **106,** 1083–1095.

Janecke, S. U. (1995a) Eocene to Oligocene half grabens of east-central Idaho: Structure, stratigraphy, age and tectonics. *Northwest Geology* **24,** 159–199.

Janecke, S. U. (1995b) Possible late Cretaceous to Eocene sediment dispersal along structurally controlled paleovalleys in the MT/ID thrust belt. *Geological Society of America Abstracts with Programs* **27,** 16.

Janecke, S. U. and Evans, J. C. (in press) Folded and faulted Salt Lake Formation above the Miocene to Pliocene (?) New Canyon and Clifton detachment faults, Malad and Bannock ranges, Idaho: Field trip guide to the Deep Creek half graben and environs. In *Guidebook for field trips for the Geological Society of America, Rocky mountain meeting,* eds S. Hughes and G. Thackery, Idaho Natural History Museum Publication.

Janecke, S. U., Hammond, B. F., Snee, L. W. and Geissman, J. W. (1997) Rapid extension in an Eocene volcanic arc: Structure and paleogeography of an intra-arc half-graben in central Idaho. *Geological Society of America Bulletin* **109,** 253–267.

Janecke, S. U., M'Gonigle, J. W., McIntosh, W. C., VanDenburg, C. J., Perry, W. J., Jr, Good, S. C. and Nichols, R. (1996a) Sedimentation patterns in the Muddy Creek, Medicine Lodge/Horse Prairie and Grasshopper supra-detachment basins, MT. *Geological Society of America Abstracts with Programs* **28,** 444.

Janecke, S. U., Perry, W. J. and M'Gonigle, J. W. (1996b) Scale dependent reactivation of pre-existing structures by an Eocene–Oligocene detachment fault, southwestern Montana. *Geological Society of America Abstracts with Programs* **28,** 78.

Janecke, S. U., VanDenburg, C. J. and Blankenau, J. J. (1998) Geometry, mechanisms, and significance of extensional folds from examples in the Rocky Mountain Basin and Range province, U.S.A. *Journal of Structural Geology* **20,** 841–856.

Kellogg, K. S., Schmidt, C. J. and Young, S. W. (1995) Basement and cover-rock deformation during Laramide contraction in the northern Madison Range (Montana) and its influence on Cenozoic basin formation. *American Association of Petroleum Geologists Bulletin* **79,** 1117–1137.

Kiilsgaard, T. H., Fisher, F. S. and Bennett, E. H. (1986) The Trans-Challis fault system and associated precious metal deposits, Idaho. *Economic Geology* **81,** 721–724.

Leeder, M. R. and Gawthorpe, R. L. (1987) Sedimentary models for extension tilt-block/half-graben basins. In *Continental Extensional Tectonics*, eds M. P. Coward, J. F. Dewey and P. L. Hancock, Vol. 28, pp. 139–152. Geological Society Special Publications.

Link, P. K. (1982) Structural Geology of the Oxford Peak and Malad Summit quadrangles, Bannock Range, southeastern Idaho. In *Geologic Studies of the Cordilleran Thrust Belt*, ed. R. B. Powers, pp. 851–858. Rocky Mountain Association of Geologists.

Liu, M. and Shen, Y. (1998) Crustal collapse, mantle upwelling, and Cenozoic extension in the North American Cordillera. *Tectonics* **17,** 311–321.

Lucchitta, B. K. (1966) Structure of the Hawley Creek area, Idaho–Montana. Ph.D. dissertation, Pennsylvania State University.

Lund, K. and Snee, L. W. (1988) Metamorphism, structural development, and age of the continent–island arc juncture in west-central Idaho. In *Metamorphism and Crustal Evolution of the Western United States, Rubey Vol. 7*, ed. W. G. Ernst, pp. 296–331. Prentice-Hall.

M'Gonigle, J. W. (1993) Geologic map of the Medicine Lodge Peak quadrangle, Beaverhead County, southwest Montana, U.S.. *Geological Survey Quadrangle Map* **GQ-1724,** scale 1:24 000.

M'Gonigle, J. W. (1994) Geologic map of the Deadman Pass quadrangle, Beaverhead county, southwest Montana, U.S. *Geological Survey Quadrangle Map* **GQ-1753,** scale 1:24 000.

M'Gonigle, J. W. and Dalrymple, G. B. (1993) $^{40}Ar/^{39}Ar$ ages of Challis volcanic rocks and the initiation of Tertiary sedimentary basins in southwestern Montana. *Mountain Geologist* **30,** 112–118.

M'Gonigle, J. W. and Dalrymple, G. B. (1996) $^{40}Ar/^{39}Ar$ ages of some Challis Volcanic Group rocks and the initiation of Tertiary sedimentary basins in southwestern Montana. *U.S. Geological Survey Bulletin* **2132**.

M'Gonigle, J. W. and Hait, M. H. (1997) Geologic map of the Jeff Davis Peak and eastern part of the Everson Creek quadrangles, Beaverhead County, southwest Montana. *U.S. Geological Survey Geologic Investigations Map* **I-2604,** scale 1:24 000.

M'Gonigle, J. W., Kirschbaum, M. A. and Weaver, J. N. (1991) Geologic map of the Hansen Ranch quadrangle, Beaverhead county, southwest Montana. *U.S. Geological Survey Geological Quadrangle Map* **GQ 1704,** scale 1:24 000.

MacCready, T., Snoke, A. W., Wright, J. E. and Howard, K. A. (1997) Mid-crustal flow during Tertiary extension in the Ruby Mountains core complex, Nevada. *Geological Society of America Bulletin* **109,** 1576–1594.

MacKenzie, W. O. (1949) Geology and ore deposits of a section of the Beaverhead Mountains east of Salmon, Idaho. M.Sc. thesis, University of Idaho.

Mancktelow, N. S. and Pavlis, T. L. (1994) Fold-fault relationships in low-angle detachment systems. *Tectonics* **13,** 668–685.

McDowell, R. J. (1992) Effects of synsedimentary basement tectonics on fold-thrust belt geometry, southwestern Montana. Ph.D. dissertation, University of Kentucky.

McDowell, R. J. (1997) Evidence for synchronous thin-skinned and basement deformation in the Cordilleran fold-thrust belt: the Tendoy Mountains, southwestern Montana. *Journal of Structural Geology* **19,** 77–87.

McIntosh, W. C. and Chamberlin, R. M. (1994) $^{40}Ar/^{39}Ar$ geochronology of Middle to Late Cenozoic ignimbrites, mafic lavas, and volcaniclastic rocks in the Quemado Region, New Mexico. *New Mexico Geological Society Guidebook,* **45,** 165–185.

McIntyre, D. H., Ekren, E. D. and Hardyman, R. F. (1982) Stratigraphic and structural framework of the Challis volcanic rocks in the eastern half of the Challis $1^\circ \times 2^\circ$ quadrangle, Idaho. In *Cenozoic Geology of Idaho*, eds B. Bonnichsen and R. M. Breckenridge, pp. 3–22. Idaho Bureau of Mines and Geology Bulletin.

Nielson, J. E. and Beratan, K. K. (1990) Tertiary basin development and tectonic implications, Whipple detachment system: Colorado River extensional corridor, Californian and Arizona. *Journal of Geophysical Research* **95,** 599–614.

O'Neill, J. M. and Lopez, D. A. (1985) Character and regional significance of the Great Falls tectonic zone, east-central Idaho and west-central Montana. *American Association of Petroleum Geologists Bulletin* **69,** 437–447.

O'Neill, R. L. and Pavlis, T. L. (1988) Superposition of Cenozoic extension on Mesozoic compressional structures in the Pioneer Mountains core complex, central Idaho. *Geological Society of America Bulletin* **100,** 1833–1845.

Perry, W. J., Jr and M'Gonigle, J. W. (1995) Neogene extensional events, northern Tendoy Mountains and adjacent Medicine Lodge

basin, southwest Montana. *Geological Society of America Abstracts with Programs* **27,** 51.

Perry, W. J. Jr and Sando, W. J. (1983) Sequential deformation in the thrust belt of southwestern Montana. In *Geologic Studies of the Cordilleran Thrust Belt*, ed. R. B. Powers, Vol. 1, pp. 137–144. Denver, Colorado, Rocky Mountain Association of Geologists.

Perry, W. J. Jr, Haley, J. C., Nichols, D. J., Hammons, P. M. and Ponton, J. D. (1988) Interactions of Rocky Mountain foreland and Cordilleran thrust belt in Lima region, southwest Montana. In *Interaction of the Mountain Foreland and the Cordilleran Thrust Belt*. eds C. J. Schmidt and W. J. Perry Jr, Geological Society of America Memoir, **171,** pp. 267–290.

Piety, L. A., Sullivan, J. T. and Anders, M. H. (1992) Segmentation and paleoseismicity of the Grand Valley fault, southeastern Idaho and western Wyoming. In *Regional Geology of Eastern Idaho and Western Wyoming*. eds P. K. Link, M. A. Kuntz and L. B. Platt. Geological Society of America Memoir, **179,** pp. 155–182.

Platt, L. B. and Royse, F. J. (1989) *The Idaho-Wyoming Thrust Belt*. American Geophysical Union, Field trip guidebook T135 28th International Geological Congress.

Ruppel, E. T. (1968) Geologic map of the Leadore quadrangle. *U.S. Geological Survey Quadrangle Map* **GQ-733,** scale 1:62 500.

Ruppel, E. T., O'Neill, J. M. and Lopez, D. A. (1993) Geologic map of the Dillon $1^\circ \times 2^\circ$ quadrangle, Idaho and Montana. *U.S. Geological Survey Miscellaneous Investigations Series Map* **I-1803-H,** scale 1:250 000.

Schlische, R. W. (1993) Anatomy and evolution of the Triassic–Jurassic continental rift system, eastern North America. *Tectonics* **12,** 1026–1042.

Schlische, R. W. (1995) Geometry and origin of fault-related folds in extensional settings. *American Association of Petroleum Geologists Bulletin* **79,** 1661–1678.

Schmidt, C. J. (1996) Neogene inversion of Cretaceous rift basins and reversion of Carboniferous uplifts in the Pampean Ranges, Argentina, with implications for reactivation in the Laramide Rocky Mountains. *Geological Society of America Abstracts with Programs* **28,** 112.

Schmidt, C. J., Evans, J. P., Harlan, S. S., Weberg, E. D., Brown, F. S., Batatian, D., Derr, D. N., Malizzi, L., McDowell, R. J., Nelson, G. C., Parke, M. and Genovese, P. W. (1993) Mechanical behavior of basement rocks during movement of the Scarface thrust, central Madison Range, Montana. In *Laramide Basement Deformation in the Rocky Mountain Foreland of the Western United States*. eds C. J. Schmidt, R. Chase and E. A. Erslev. Geological Society of America Special Paper, **280,** pp. 89–105.

Schmidt, C. J., Sheedlo, M. and Werkema, M. (1984) Control of range-boundary normal faults by earlier structure, southwestern Montana. *Geological Society of America Abstracts with Programs* **16,** 253.

Scholten, R. and Ramspott, L. D. (1968) Tectonic mechanisms indicated by structural framework of central Beaverhead Mountains, Idaho–Montana. *Geological Society of America Special Paper* **104,** 70 pp.

Scholten, R., Keeman, K. A. and Kupsch, W. O. (1955) Geology of the Lima region, southwestern Montana and adjacent Idaho. *Geological Society of America Bulletin* **66,** 345–404.

Scott, W. E., Pierce, K. L. and Hait, M. J., Jr (1985) Quaternary tectonic setting of the 1983 Borah Peak earthquake, central Idaho. *Bulletin of the Seismological Society of America* **75,** 1053–1066.

Sears, J. W. (1995) Middle Miocene rift system in SW Montana: Implications for the initial outbreak of the Yellowstone hot spot: Geologic history of the Dillon area, southwestern Montana. *Northwest Geology* **25,** 43–46.

Sears, J. W. and Fritz, W. J. (1998) Cenozoic tilt domains in southwestern Montana: Interference among three generations of extensional fault systems. In *Accomodation zones and transfer zones: The regional segmentation of the Basin and Range province,* eds J. E. Faulds and J. H. Stewart. Geological Society of America Special Paper, **323,** pp. 241–249.

Sears, J. W., Hurlow, H., Fritz, W. J. and Thomas, R. C. (1995) Late Cenozoic disruption of Miocene grabens on the shoulder of the Yellowstone hot spot track in southwest Montana: Field guide from Lima to Alder, Montana. *Northwest Geology* **24,** 201–219.

Serpa, L. and Pavlis, T. L. (1996) Three-dimensional model of the Cenozoic history of the Death Valley region, southeastern California. *Tectonics* **15,** 1113–1128.

Sharp, W. N. and Cavender, W. S. (1962) Geology and thorium-bearing deposits of the Lemhi Pass area, Lemhi County, Idaho, and Beaverhead County, Montana. *U.S. Geological Survey Bulletin* **1126**.

Silverberg, D. S. (1990) Denudation rates & timing of diachronous Paleogene extension in south-central Idaho. *Geological Society of America Abstracts with Programs* **22,** 330.

Skipp, B. (1984) Geologic map and cross-sections of the Italian Peak and Italian Peak Middle Roadless areas, Beaverhead County, Montana, and Clark and Lemhi Counties, Idaho. *U.S. Geological Survey Miscellaneous Field Studies Map* **MF-1061-B,** scale 1:62 500.

Skipp, B. (1987) Basement thrust sheets in the Clearwater orogenic zone, central Idaho and western Montana. *Geology* **15,** 220–224.

Skipp, B. (1988) Cordilleran thrust belt and faulted foreland in the Beaverhead Mountains, Idaho and Montana. In *Interaction of the Rocky Mountain Foreland and Cordilleran Thrust Belt*. eds C. J. Schmidt and W. J. Perry Jr. Geological Society of America Memoir, **171,** pp. 237–266.

Smith, K. A. (1997) Stratigraphy, geochronology, and tectonics of the Salt Lake Formation (Tertiary) of southern Cache Valley, Utah. M. Sc. thesis, Utah State University.

Smith, K. A., Oaks, R. Q., Jr and Janecke, S. U. (1997) N-trending folds and ENE-striking normal faults postdate 5.1 Ma Salt Lake Formation and predate peidment, Cache Valley Utah, NE Basin-and-Range province. *Geological Society of America Abstracts with Program* **29,** 349.

Snider, L. G. (1995) Stratigraphic framework, geochemistry, geochronology, and eruptive styles of Eocene volcanic rocks in the White Knob Mountains area, southeastern Challis volcanic field, central Idaho. M.Sc. thesis, Idaho State University.

Staatz, M. H. (1973) Geologic map of the Goat Mountain quadrangle, Lemhi County, Idaho and Beaverhead County, Montana. *U.S. Geological Survey Quadrangle Map* **GQ-1097**.

Staatz, M. H. (1979) Geology and mineral resources of the Lemhi Pass thorium district, Idaho and Montana. *U.S. Geological Survey Professional Paper* **1049-A**.

Stickney, M. C. and Bartholomew, M. J. (1987) Seismicity and Quaternary faulting of the northern Basin and Range Province, Montana and Idaho. *Bulletin of the Seismological Society of America* **77,** 1602–1625.

Taylor, W. J., Bartley, J. M., Lux, D. R. and Axen, G. J. (1989) Timing of extension in the Railroad valley–Pioche transect, Nevada: Constraints from $^{40}Ar/^{39}Ar$ ages of volcanic rocks. *Journal of Geophysical Research* **94,** 7757–7774.

Tucker, D. R. (1975) Stratigraphy and structure of Precambrian Y (Belt?) metasedimentary and associated rocks, Goldstone Mountain quadrangle, Lemhi County, Idaho, and Beaverhead County, Montana. Ph.D. dissertation, Miami University.

Tysdal, R. G. (1996a) Geologic map of the Lem Peak quadrangle, Lemhi County, Idaho. *U.S. Geological Survey Quadrangle Map* **GQ-1777,** scale 1:24 000.

Tysdal, R. G. (1996b) Geologic map of adjacent areas in the Hayden Creek and Mogg Mountain quadrangles, Lemhi County, Idaho. *U.S. Geological Survey Miscellaneous Investigations Series Map* **I-2563,** scale 1:24 000.

Tysdal, R. G. and Moye, F. J. (1996) Geologic map of the Allison Creek quadrangle, Lemhi County, Idaho. *U.S. Geological Survey Quadrangle Map* **GQ-1778,** scale 1:24 000.

VanDenburg, C. J. (1997) Cenozoic tectonic and paleogeographic evolution of the Horse Prairie half graben, southwest Montana. M.Sc. thesis, Utah State University.

Wells, M. L. (1997) Alternating contraction and extension in the hinterlands of orogenic belts: An example from the Raft River Mountains, Utah. *Geological Society of America Bulletin* **109,** 107–126.

Wernicke, B. (1992) Cenozoic extensional tectonics of the U.S. Cordillera. In *The Cordilleran Orogen: Conterminous U.S. Geology of North America*. eds B. C. Burchfield, P. W. Lipman and M. L. Zoback. Geological Society of America. G-3. pp. 553–682.

Yin, A. and Dunn, J. F. (1992) Structural and stratigraphic development of the Whipple–Chemehuevi detachment fault system, southeastern California: Implications for the geometrical evolution of

domal and basinal low angle normal faults. *Geological Society of America Bulletin* **104,** 659–674.

Zheng, J. (1996) Paleomagnetism and magnetostratigraphy of the Miocene Railroad Canyon Formation, Idaho. Ph.D. dissertation, University of Pittsburg.

Ziegler, P. A. and van Hoorn, B. (1989) Evolution of North Sea rift system. In *Extensional Tectonics and Stratigraphy of the North Atlantic Margins*, eds A. J. Tankard and H. R. Balkwill, pp. 471–500. American Association of Petroleum Geologists Memoir, **46**.

Zoback, M. L., Anderson, R. E. and Thompson, G. A. (1981) Cainozoic evolution of the state of stress and style of tectonism of the Basin and Range province of the western United States. *Philosophical Transactions of the Royal Society of London* **300,** 189–216.